

SLANTLET TRANSFORM-BASED SEGMENTATION AND α -SHAPE
THEORY-BASED 3D VISUALIZATION AND VOLUME CALCULATION
METHODS FOR MRI BRAIN TUMOUR

MOHAMMED SABBIH HAMOUD AL-TAMIMI

A thesis submitted in fulfilment of the
requirements for the award of the degree of
Doctor of Philosophy (Computer Science)

Faculty of Computing
Universiti Teknologi Malaysia

NOVEMBER 2015

I would like to dedicate this work for
my beloved wife "Hala" and lovely kids
"Malak & Hussein"
for being patience, supportive, and understanding.

ACKNOWLEDGEMENT

Thanks to Allah SWT for everything I was able to achieve and for everything I tried, but I was not able to achieve.

To my supervisor *Professor Dr. Ghazali Bin Sulong*, you are truly a SUPER-visor. I am greatly appreciative of him for his support and guidance, most importantly, for providing me the freedom to pursue my ideas and find my own path in research. Also, I have gained a wealth of experience and knowledge working under your supervision, which will always be my delight to share along my life's journey. Thanks also to Consultant Radiologists, *Professor Dr. Ibrahim Shuaib*, and *Dr. Zahari Mahbar* for their involvement in this research.

To my beloved father, *Professor Dr. Sabbih H. Al-Tamimi*, thank you for bringing a side of me. I will always cherish your limitless support and encouragement.

To all my *family* and *DR. Safaa Najah Saud*, receives my deepest gratitude and love for their patience and support during the years of my study.

ABSTRACT

Magnetic Resonance Imaging (MRI) being the foremost significant component of medical diagnosis which requires careful, efficient, precise and reliable image analyses for brain tumour detection, segmentation, visualisation and volume calculation. The inherently varying nature of tumour shapes, locations and image intensities make brain tumour detection greatly intricate. Certainly, having a perfect result of brain tumour detection and segmentation is advantageous. Despite several available methods, tumour detection and segmentation are far from being resolved. Meanwhile, the progress of 3D visualisation and volume calculation of brain tumour is very limited due to absence of ground truth. Thus, this study proposes four new methods, namely abnormal MRI slice detection, brain tumour segmentation based on Slantlet Transform (SLT), 3D visualization and volume calculation of brain tumour based on Alpha (α) shape theory. In addition, two new datasets along with ground truth are created to validate the shape and volume of the brain tumour. The methodology involves three main phases. In the first phase, it begins with the cerebral tissue extraction, followed by abnormal block detection and its fine-tuning mechanism, and ends with abnormal slice detection based on the detected abnormal blocks. The second phase involves brain tumour segmentation that covers three processes. The abnormal slice is first decomposed using the SLT, then its significant coefficients are selected using Donoho universal threshold. The resultant image is composed using inverse SLT to obtain the tumour region. Finally, in the third phase, four original ideas are proposed to visualise and calculate the volume of the tumour. The first idea involves the determination of an optimal α value using a new formula. The second idea is to merge all tumour points for all abnormal slices using the α value to form a set of tetrahedrons. The third idea is to select the most relevant tetrahedrons using the α value as the threshold. The fourth idea is to calculate the volume of the tumour based on the selected tetrahedrons. In order to evaluate the performance of the proposed methods, a series of experiments are conducted using three standard datasets which comprise of 4567 MRI slices of 35 patients. The methods are evaluated using standard practices and benchmarked against the best and up-to-date techniques. Based on the experiments, the proposed methods have produced very encouraging results with an accuracy rate of 96% for the abnormality slice detection along with sensitivity and specificity of 99% for brain tumour segmentation. A perfect result for the 3D visualisation and volume calculation of brain tumour is also attained. The admirable features of the results suggest that the proposed methods may constitute a basis for reliable MRI brain tumour diagnosis and treatments.

ABSTRAK

Pengimejan Resonans Magnetik (MRI) merupakan komponen utama yang penting dalam diagnostik perubatan yang memerlukan analisis imej yang teliti, cekap, tepat dan diyakini untuk pengesanan, segmentasi, visualisasi dan pengiraan isipadu tumor otak. Sememangnya tumor mempunyai pelbagai bentuk, lokasi dan keamatan imej yang sangat merumitkan bagi pengesananannya. Tentunya, adalah amat berfaedah jika sekiranya hasil pengesanan dan segmentasi tumor otak yang sempurna dapat diperolehi. Walaupun terdapat beberapa kaedah yang tersedia, namun pengesanan tumor dan segmentasi masih lagi belum dapat diselesaikan sepenuhnya. Sementara itu, kemajuan visualisasi 3D dan pengiraan isipadu tumor otak adalah sangat terhad kerana ketiadaan kebenaran mutlak. Oleh itu, kajian ini mencadangkan empat kaedah baharu iaitu pengesanan hirisan MRI tidak normal, segmentasi tumor otak berdasarkan jelmaan Slantlet (SLT), visualisasi 3D dan pengiraan isipadu tumor otak berdasarkan teori bentuk Alpha (α). Di samping itu, dua set data baharu beserta dengan kebenaran mutlak telah dicipta untuk mengesahkan bentuk dan isipadu tumor otak. Metodologi ini melibatkan tiga fasa utama. Dalam fasa pertama, ia dimulai dengan pengekstrakan tisu otak, diikuti dengan pengesanan blok yang tidak normal dan mekanisme penalaan halus, dan berakhir dengan pengesanan hirisan yang tidak normal berdasarkan blok tidak normal yang telah dikesan. Fasa kedua melibatkan segmentasi tumor otak yang merangkumi tiga proses. Pertama, hirisan tidak normal diuraikan menggunakan SLT, kemudian pekalinnya yang signifikan dipilih menggunakan ambang sejagat Donoho. Imej yang terhasil dibentuk menggunakan SLT songsang untuk mendapatkan kawasan tumor. Akhirnya, dalam fasa ketiga, empat idea asli dicadangkan untuk menggambarkan dan mengira isipadu tumor. Idea pertama, ia melibatkan penentuan nilai α optimum secara automatik menggunakan satu formula baharu. Idea kedua adalah untuk menggabungkan semua titik tumor bagi kesemua hirisan tidak normal menggunakan nilai α tersebut untuk membentuk satu set tetrahedron. Idea ketiga adalah untuk memilih tetrahedron yang paling sesuai menggunakan nilai α di atas sebagai nilai ambang. Idea keempat adalah untuk mengira isipadu tumor berdasarkan tetrahedron yang terpilih. Dalam usaha untuk menilai prestasi kaedah-kaedah yang dicadangkan, satu siri eksperimen dijalankan menggunakan tiga set data piawai yang merangkumi 4567 hirisan MRI daripada 35 pesakit. Kaedah-kaedah tersebut dinilai dengan menggunakan amalan piawai serta ditanda araskan dengan teknik-teknik terkini yang terbaik. Berdasarkan eksperimen, kaedah-kaedah yang dicadangkan telah menghasilkan keputusan yang sangat menggalakkan dengan kadar ketepatan 96% bagi pengesanan keabnormalan hirisan dan 99% sensitiviti dan spesifisiti untuk segmentasi tumor otak. Keputusan yang sempurna juga dicapai bagi visualisasi 3D dan pengiraan isipadu tumor otak. Ciri-ciri yang mengkagumkan daripada keputusan ini mencadangkan bahawa kemungkinan kaedah-kaedah yang dicadangkan ini boleh dijadikan asas yang dipercayai bagi diagnosis tumor otak MRI dan rawatan.

TABLE OF CONTENTS

CHAPTER	TITLE	PAGE
	DECLARATION	ii
	DEDICATION	iii
	ACKNOWLEDGEMENT	iv
	ABSTRACT	v
	ABSTRAK	vi
	TABLE OF CONTENTS	vii
	LIST OF TABLES	xiii
	LIST OF FIGURES	xvi
	LIST OF ABBREVIATIONS	xxxi
	LIST OF SYMBOLS	xxxiv
	LIST OF ALGORITHMS	xxxvi
	LIST OF APPENDICES	xxxviii
1	INTRODUCTION	1
1.1	Overview	1
1.2	Designations	3
1.3	Background of Research	6
1.4	Problem Statements	13
1.5	Research Goal	15
1.6	Objectives of the Study	15
1.7	Research Scope	15
1.8	Significance of the Study	16
1.9	Thesis Outline	17

2	LITERATURE REVIEW	19
2.1	Introduction	19
2.2	Medical Glossary of Brain Tumour	20
2.2.1	Brain Anatomy	21
2.2.2	Brain Tumour	23
2.2.3	MRI Brain Imaging	24
2.3	Detetection Abnormal Slices in Magnetic Resonance Images	25
2.3.1	Cerebral Tissues Extraction	26
2.3.1.1	Cerebral Tissues Extraction Based on Intensity	28
2.3.1.2	Cerebral Tissues Extraction Based on Morphology	29
2.3.1.3	Cerebral Tissues Extraction Based on Deformation	30
2.3.2	Classification Methods for Detecting Abnormality in Brain MR Images	32
2.4	Medical Image Segmentation	34
2.4.1	Spatial Clustering	36
2.4.2	Split and Merge Segmentation	36
2.4.3	Region Growing	37
2.4.4	Computational Techniques for Medical Image Segmentation	37
2.4.4.1	Thresholding Based Methods	38
2.4.4.2	Region Growing Based Methods	40
2.4.4.3	Neural Networks Based Methods	43
2.4.4.4	Fuzzy Based Methods	45
2.4.4.5	Hybrid Techniques	49
2.4.4.6	Other Brain Tumour Segmentation and Detection	52

	Techniques	
2.5	Volumetric Calculation and 3D Visualization of Brain Tumour in MRI	57
2.6	Alpha (α) Shape Theory	59
2.6.1	Modelling and Visualization Using α -Shape Theory	62
2.6.2	Limitations of α -Shape	63
2.6.3	Determination of the Best α Value	65
2.6.3.1	Small α Values Selection	65
2.6.3.2	Large α Values Selection	67
2.6.3.3	Selecting α Value “Just Right”	67
2.7	Summary	68
3	A CONCEPTUAL FRAMEWORK	70
3.1	Introduction	70
3.2	Research Framework	71
3.3	Operational Research Framework	74
3.4	Validation of the Proposed Methods	77
3.4.1	Quantitative Evaluation	78
3.4.1.1	Jaccard and Dice Coefficients	79
3.4.1.2	Sensitivity, Specificity and Accuracy	80
3.4.2	Qualitative Evaluation	81
3.5	Benchmarking	82
3.5.1	Frustum Model	83
3.5.2	Meshing Point Clouds	83
3.5.3	Trace Method	83
3.5.4	Modified MacDonald (MMC) Method	84
3.6	Dataset	85
3.6.1	IBSR (10Normals_T1) Dataset	87
3.6.2	IBSR (536_T1) Dataset	89
3.6.3	Challenge MICCAI (BRATS2012-BRATS-1) Dataset	92

3.7	Creation of Two Ground Truth	95
3.8	Summary	105
4	DESIGN AND IMPLEMENTATION OF PROPOSED METHOD	107
4.1	Introduction	107
4.2	Detection of Abnormal MRI Slices	108
4.2.1	Extraction of the Cerebral Tissues	109
4.2.1.1	Image Binarization	111
4.2.1.2	Largest Connected Component	113
4.2.1.3	Masking	118
4.2.1.4	Bitwise Operation “AND”	119
4.2.2	Determination of Thresholds	121
4.2.2.1	Features Extraction	124
4.2.2.2	Mean, Energy and Entropy Distribution	126
4.2.2.3	Mean, Energy and Entropy Correlation	131
4.2.3	Detection of Abnormal Blocks	134
4.3.2.1	Fine-tuning of Abnormal Blocks	135
4.3	Automatic Segmentation of Brain Tumour Based on Slantlet Transform	142
4.3.1	Slantlet Transform Decomposition	143
4.3.2	Selection of Significant SLT Coefficients	154
4.3.3	Inverse Slantlet	157
4.4	3D Visualization and Volumetric Measurement of Brain Tumour Based on α -Shape Theory	160
4.4.1	Extraction of Tumour Point	162
4.4.2	Determination of the α Value	163
4.4.3	Assembly of Tumour Cloud Points	166

	Using α -Shapes Theory	
	4.4.3.1 Construction of α -Shapes	166
	4.4.3.2 Delaunay Triangulation	167
	4.4.3.3 Implementation of Delaunay Triangulation	170
	4.4.3.4 α -Shapes Implementation	178
	4.4.4 Brain Tumour 3D Visualization and Volume Calculation	182
4.5	Summary	183
5	QUALITATIVE AND QUANTITATIVE EXPERIMENTAL RESULT	184
5.1	Introduction	184
5.2	Result of Abnormal Slice Detection	186
5.2.1	Results of Cerebral Tissue Extraction	186
5.2.2	Results of the Abnormal Block Detection Before the Fine-tuning	190
5.2.3	Results of the Fine-tuning of Abnormal Block detection	197
5.2.4	The Quantitative Assessment of the Tumour Block Detection	207
5.2.4.1	Quantitative Evaluation of Slice Abnormality Detection	215
5.3	Performance Evaluation of the Proposed SLT-based Segmentation Technique	221
5.3.1	Results and Discussions of the Qualitative Evaluation	222
5.3.2	Results and Discussions of the Quantitative Evaluation	228
5.4	Performance Evaluation of 3D Visualization and Volume Calculation of Brain Tumours	235
5.4.1	Qualitative Evaluation of 3D Visualization of Brain Tumour	235

5.4.2	Quantitative Evaluation of Brain Tumour Volume Calculation	250
5.5	Summary	256
6	CONCLUSIONS AND FURTHER OUTLOOK	258
6.1	Contributions	261
6.2	Further Outlook	263
	REFERENCES	265
	Appendices A-C	293-300

LIST OF TABLES

TABLE NO.	TITLE	PAGE
2.1	Relevant literatures on thresholding based methods	39
2.2	Relevant literatures on region growing based methods	41
2.3	Relevant literatures on NN based methods	45
2.4	Relevant literatures on Fuzzy based methods	47
2.5	Relevant literatures on Hybrid techniques	50
2.6	Relevant literatures on other brain tumour segmentation and detection techniques	53
3.1	Summary of the operational research framework	75
3.2	Validation of the proposed methods	77
3.3	Definition of TP, TN, FN, and FP	80
3.4	Existing methods for benchmarking of different processes	82
3.5	Properties of normal patient from IBSR (10Normals_T1) dataset	89
3.6	Properties of abnormal patient from IBSR (536_T1) dataset	92
3.7	Properties of challenge MICCAI (BRATS2012-BRATS-1) dataset	95
3.8	Hitachi Airs MRI device specifications	98
3.9	The computer specifications of Hitachi Airs MRI device	99
3.10	The mass of the six irregular objects	102

3.11	Calculation of displaced water weight of the six irregular objects	104
3.12	The ground truth volume of all irregular objects (solid and hollow)	105
4.1	The pixel count of each region in MRI slice “T”	116
4.2	The threshold values of mean, energy and entropy for the different datasets	134
4.3	ROI dimension according to SLT filter-bank	149
4.4	The values of slice thickness and pixel spacing of MR images from different sources	163
5.1	Block abnormality detection results of the IBSR (10Normals_T1) dataset	208
5.2	Block abnormality detection results of the IBSR (536_T1) dataset	211
5.3	Block abnormality detection results of the challenge MICCAI (BRATS2012-BRATS-1) dataset	213
5.4	Experimental results of slice abnormality detection of IBSR (10Normals_T1) dataset	216
5.5	Experimental results of abnormality detection by slice obtained from the IBSR (536_T1) dataset.	217
5.6	Experimental results of abnormality detection by slice obtained from the challenge MICCAI (BRATS2012-BRATS-1) dataset	218
5.7	Jaccard and Dice indices of the proposed method implemented on the IBSR (536_T1) dataset	228
5.8	Jaccard and Dice indices of the proposed method implemented on the challenge MICCAI (BRATS2012-BRATS-1) dataset	229
5.9	Sensitivity, specificity, and accuracy of the proposed segmentation method implemented on IBSR (536_T1) dataset	230
5.10	Sensitivity, specificity, and accuracy of the proposed segmentation method implemented on challenge MICCAI (BRATS2012-BRATS-1)	232

5.11	Performance results of the proposed method versus the state-of-the-art techniques for the challenge MICCAI (BRATS2012-BRAT-1) dataset	233
5.12	Calculated volume of the six objects	251
5.13	The proposed method versus four standard volume measures in terms volume error rates of six irregular objects	252
5.14	Calculated tumour volumes of IBSR (536_T1) dataset: Comparison between the proposed method and the four standard measures	254
5.15	Calculated tumour volumes of challenge MICCAI (BRATS2012-BRATS-1) dataset: Comparison between the proposed method and the four standard measures	255

LIST OF FIGURES

FIGURE NO	TITLE	PAGE
1.1	Human brain slices with different imaging modalities. From left to right: CT, MRI, SPECT and PET (Wright 2010)	4
1.2	MR brain image from patient's head (a) The setup, (b) Axial plane view, (c) Sagittal plane view, and (d) Coronal plane view (Lorenzen <i>et al.</i> 2001)	5
1.3	MR image sequence (Brown and Semelka 2011)	6
1.4	Normal MRI slices from IBSR (10Normals_T1) dataset, (a) Slice 22 of patient Normal_4, and (b) Slice 16 of patient Normal_15	7
1.5	Normal MRI slices from challenge MICCAI (BRATS2012-BRATS-1) dataset, (a) Slice 119 of patient BRATS_HG0010, and (b) Slice 54 of patient BRATS_HG0008	8
1.6	Abnormal MRI slices at different locations with varying size, shapes, and image intensities of brain tumour (red rectangle) from IBSR (536_T1) dataset of MRI scan 536_32, (a) Slice 22, and (b) Slice 26	8
1.7	Abnormal MRI slices in the presence of tumour inside the red square in terms of intensity homogeneity from challenge MICCAI (BRATS 2012-BRATS-1) dataset, (a) Slice 85 of patient	

	BRATS_HG0004, and (b) Slice 127 of patient BRATS_HG0007	9
1.8	3D brain tumour visualization of MRI scan 536_32 in IBSR (536_T1) dataset using Matlab's Meshing Point Clouds function	10
2.1	GM and WM brain tissues (Nolte 2013)	21
2.2	Normal circulation of CSF in the brain (Nolte 2013)	22
2.3	Major subdivision of human brain (Nolte 2013)	22
2.4	The working principle of MRI machine (Dominik <i>et al.</i> 2008)	25
2.5	Slice 44 of MRI scan 536_88 in IBSR (536_T1) dataset, (a) with non-cerebral tissues, and (b) without non-cerebral tissues	27
2.6	Typical results of cerebral tissues extraction, (a) Original MR image, (b) WAT extracted image (Sadananthan <i>et al.</i> 2010)	28
2.7	Typical results of BSE cerebral tissues extraction, (a) Original MR image, (b) BSE extracted image (Sadananthan <i>et al.</i> 2010)	29
2.8	Typical results of BET cerebral tissues extraction, (a) Original MR image, (b) BET extracted image	31
2.9	Typical results of HWA cerebral tissues extraction, (a) Original MR image, (b) HWA extracted image (Sadananthan <i>et al.</i> 2010)	31
2.10	(a) original image, (b) ground truth-based border image, (c) seeded image; (d) and (e) are segmentation results using the RGB a colour space presenting their best index; (f) and (g) are segmentation results using the adaptive discrimination function generated by the seed points presented in (c) with best rand index (Haralick and Shapiro 1985)	35

2.11	Same set of points with: a) linear frontier, b) convex hull, c) concave hull, and d) α -Shape	61
2.12	Examples of 3D model to form mesh of triangular faces using α -shape theory	62
2.13	The interstice problem, (a) Break in the object surface, (b) Wrong interstice close using α -shape, and (c) Right interstice close	63
2.14	Demonstration of the failure between surfaces at joints and interstices (a) Two separate objects, and (b) Wrong joint using α -shape, and (c) Right joint close	64
2.15	α -shape with different values: (a) $\alpha = 0$, (b) $\alpha = 0.19$, (c) $\alpha = 0.25$, (d) $\alpha = 0.75$, (e) $\alpha = \infty$	64
2.16	A set of points representing the locations of bus stations in a town	65
2.17	The α -shape created from the bus stations using $\alpha = 0.5$ KM	66
2.18	The α -shape created from the bus stations using $\alpha = 3$ KM	67
2.19	The α -shape created from the bus stations using $\alpha = 1.1$ KM	68
3.1	An overview of the proposed methodology	72
3.2	The detection / segmentation in MRI slices using Jaccard and Dice coefficients	79
3.3	Two longest orthogonal diameters of the largest tumours for MRI scan 536_88 in IBSR (536_T1) dataset, (a) Original slice 28, (b) Tumour segmentation, (c) diameter d_1 (blue line), and (d) diameter d_2 (green line)	85
3.4	Three MRI datasets used in the present research	86
3.5	3D views of 56 MRI slice of the patient Normal_8 living brain obtained from IBSR (10Normals_T1) dataset	88

3.6	3D views of sixty MRI slices of the MRI scan 536_32 living brain obtained from IBSR (536_T1) dataset	90
3.7	The ground truth of 3D views for sixty MRI slices of the MRI scan 536_32 living brain obtained from IBSR (536_T1) dataset	91
3.8	3D views of 176 MRI slice of the patient's living brain obtained from challenge MICCAI (BRATS2012-BRATS-1) dataset	93
3.9	The ground truth of 3D views of 176 MRI slice of the patient's living brain obtained from challenge MICCAI (BRATS2012-BRATS-1) dataset	94
3.10	Four irregular solid objects (a) Meat, (b) Carrot, (c) Egg, and (d) Cucumber	96
3.11	Irregular object with cavity, (a) Potato, and (b) Green Pepper	96
3.12	The MRI scan process of six irregular objects	97
3.13	2006 Hitachi Airis Elite 0.3T Open MRI	97
3.14	The MRI scan of an egg, (a) MR slices images, and (b) MR slices with segmented egg images	99
3.15	The MRI scan of a potato, (a) MR slices of egg images, and (b) MR slices with segmented potato images	100
3.16	Mettler AT400 balance	101
3.17	The mass calculation of (a) Green Pepper, (b) Potato, (c) Cucumber, (d) Egg, (e) Carrot, and (f) Meat	102
3.18	Beaker glass of volume (a) 1000 ml, and (b) 250 ml	103
3.19	Water displacement calculations, (a) Green pepper, (b) Egg, (c) Potato, (d) Carrot, (e) Meat, and (f) Cucumber	104
4.1	Flowchart of the proposed method for the detection of abnormal MRI slices	109

4.2	The proposed method for extraction cerebral tissues from MRI slices	111
4.3	A sample of binary MRI slice	114
4.4	Four detected regions (1 to 4) of a binary MRI slice	115
4.5	The largest region or the detected LCC	116
4.6	Detected LCC in MRI scan 536_32 of IBSR (536_T1) dataset, (a) Slice 14, (b) Slice 37, (c) Slice 45, and (d) Slice 52	117
4.7	The connected components of MRI scan 536_32 in IBSR (536_T1) data set, (a) Original slice 9, and (b) Three different connected components (red, green, and blue)	120
4.8	The cerebral tissue extraction of MRI scan 536_32 in IBSR (536_T1) dataset, (a) Original slice 9, (b) Binary image with three connected components (white regions), (c), the LCC (the largest white region), (d) the LCC mask (black region), and (e) Extracted cerebral tissue	120
4.9	The probability of the tumour occurrence in MR image slices for IBSR (536_T1) dataset	122
4.10	Tumour occurrence probability in MR image slices for challenge MICCAI (BRATS2012-BRATS-1) dataset	123
4.11	Non-overlapping block partition of patient Normal_19 of IBSR (10Normals_T1) dataset, (a) Original slice 23, and (b) Non-overlapping block division using (8×8) block size	124
4.12	Non-overlapping block partition of patient BRATS_HG0009 of challenge MICCAI (BRATS2012-BRATS-1) dataset, (a) Original slice 103, and (b) Non-overlapping block division using (8×8) block size	125
4.13	Non-overlapping block division of slice 88 for	127

	patient BRATS_HG0015 of challenge MICCAI (BRATS2012-BRATS-1) dataset using (8×8) block size	
4.14	Manual identification of slice 88 for patient BRATS_HG0015 of challenge MICCAI (BRATS2012-BRATS-1) dataset into Normal (N) and Abnormal (A) regions	128
4.15	Distribution of mean of slice 88 for patient BRATS_HG0015 of challenge MICCAI (BRTAS2012-BRATS-1) dataset	129
4.16	Distribution of entropy of slice 88 for patient BRATS_HG0015 of challenge MICCAI (BRTAS2012-BRATS-1) dataset	129
4.17	Distribution of energy of slice 88 for patient BRATS_HG0015 of challenge MICCAI (BRTAS2012-BRATS-1) dataset	130
4.18	Relation among mean, energy, and entropy of slice 88 for patient BRATS_HG0015 of challenge MICCAI (BRTAS2012-BRATS-1) dataset	131
4.19	The relationship between mean and energy of slice 88 for patient BRATS_HG0015 in challenge MICCAI (BRTAS2012-BRATS-1) dataset	132
4.20	The relationship between entropy and energy of slice 88 for patient BRATS_HG0015 in challenge MICCAI (BRTAS2012-BRATS-1) dataset	132
4.21	The relationship between entropy and mean of slice 88 for patient BRATS_HG0015 in challenge MICCAI (BRTAS2012-BRATS-1) dataset	133
4.22	Abnormal block detections rules	134
4.23	Three types of block masks with size (3×3) called preceding mask centred at P_i , current mask centred at C_i , and succeeding mask centred at S_i . Green colour indicates ignored block	136
4.24	The framing blocks (yellow blocks) of slice 90 for	136

	patient BRATS_HG0011 in challenge MICCAI (BRATS2012-BRATS-1) dataset	
4.25	Fine-tuning of Case 1: $(a_1) \rightarrow (a_2)$, and Case 2: $(b_1) \rightarrow (b_2)$, where the mechanism changes the block C_i based on its neighbours	137
4.26	Fine-tuning of (Case 3 - Case 6), where C_i is changed from tumour to a non-tumour block using the Rule 1	138
4.27	Fine-tuning of (Case 7 - Case 10), where C_i is changed from non-tumour to a tumour block using the Rule 2	139
4.28	Fine-tuning of (Case 11 - Case 14), where C_i became a non-tumour block using the Rule 3	140
4.29	The conventional 2D SLT decomposition schemes for dividing an image	144
4.30	The SLTimage matrix operation	153
4.31	The SLTimage for MRI scan 536_32 in IBSR (536_T1) dataset, (a) Original slice 25, (b) Collection of tumour blocks (ROI), and (c) SLTimage (SLT coefficient matrix of ROI)	154
4.32	Replacement of all insignificant coefficients of SLTimage of slice 25 of MRI scan 536_32 of IBSR (536_T1) dataset, (a) SLTimage before zeroing, and (b) Final SLTimage after zeroing all insignificant coefficients	157
4.33	The SLT matrix operation	158
4.34	ISLT composition of slice 25 of MRI scan 536_32 of IBSR (536_T1) dataset, (a) SLTimage after zeroing all insignificant coefficients, and (b) The final segmented MRI slice composed by ISLT	160
4.35	Flowchart of 3D visualization and volume calculation of the brain tumour using the proposed method	161

4.36	Duplication of MRI slices: Original slice in black frame and duplicated slice in red frame	164
4.37	Different triangulations of the same a set of points	167
4.38	Triangulation of set of 10 points (a) set of 10 points, and (b) Eleven DTs	168
4.39	A circumcircle of a set of points	168
4.40	An example of DT, (a) Set of points, (b) a DT, (c) a non-DT, and (d) four DTs	169
4.41	Set of points of convex body (dotted line) with P located inside	171
4.42	Q is the nearest point of the convex body	171
4.43	Determination of the third point R (largest angle) to form a DT from a set neighbouring points of P and Q	172
4.44	A formation of the first DT emanating from P	172
4.45	Formation of the second triangle with PR line as the reference line	173
4.46	Formation of the second DT emanating from P	173
4.47	Five DTs emanating from P	174
4.48	Set of points where P is located on a convex hull body (dotted lines)	175
4.49	Q is the nearest neighbour to P	175
4.50	Two triangles emanating from P with its right	176
4.51	Two triangles emanating from P with its left side	176
4.52	Four DTs emanating from P	177
4.53	A tetrahedron with six edges and four vertices	179
4.54	A circumsphere of the tetrahedron	179
4.55	The height and area of tetrahedron	180
4.56	A final collection of the Tetrahedrons: (a) Original collection of the tetrahedrons, (b) Collection of tetrahedrons with the omitted one (green line), and (c) Final collection of tetrahedrons after the α -Shapes implementation	182

5.1	General framework of the performance evaluation	185
5.2	The original slice 14 of MRI scan 536_32 in IBSR (536_T1) dataset showing cerebral and non-cerebral tissues	187
5.3	Results on cerebral tissue extraction for slice 14 of MRI scan 536_32 in IBSR (536_T1) dataset	187
5.4	Results of cerebral tissue extraction from IBSR (536_T1) dataset	189
5.5	Abnormal block detection results of MRI slices of IBSR (10Normals_T1) dataset	190
5.6	Abnormal block detection results of MRI slice of IBSR (536_T1) dataset with tumour marked by a red circle	191
5.7	Abnormal block detection results of MRI slices of challenge MICCAI (BRATS2012-BRAST-1) dataset with tumour marked by a red circle	192
5.8	Misclassified blocks of MRI slices of IBSR (10Normals_T1) dataset without any tumour	194
5.9	Misclassified blocks of MRI slices of IBSR (536_T1) dataset with tumour marked via green circle	195
5.10	Misclassified blocks of MRI slices of challenge MICCAI (BRATS2012-BRATS-1) dataset with tumour marked via green circle	196
5.11	A fine-tuning result of tumour block of slice 13 of patient Normal_7 of IBSR (10Normal_T1) dataset: (a) The original non-tumour slice 13 (in grid), (b) Fine-tuning of misclassified block of the current slice, and (d) Final result of the questioned block	198
5.12	A fine-tuning result of tumour block of slice 21 of patient Normal_17 of IBSR (10Normal_T1) dataset: (a) The original non-tumour slice 21 (in grid), (b) Fine-tuning of the misclassified block of	199

- the current slice, and (d) Final result of the questioned block
- 5.13 A fine-tuning result of three tumour blocks of slice 30 of patient Normal_17 of IBSR (10Normal_T1) dataset: (a) The original non-tumour slice 30 (in grid), (b) Fine-tuning of the misclassified blocks of the current slice, and (c) Final results of the questioned block 200
- 5.14 A fine-tuning result of two tumour blocks of slice 28 of MRI scan 536_45 from IBSR (536_T1) dataset: (a) The original tumour slice 28 (in grid), (b) Fine-tuning of the misclassified blocks of the current slice, and (c) Final result of the questioned blocks 201
- 5.15 A fine-tuning result of six tumour blocks (two separate locations) of slice 21 of MRI scan 536_47 from IBSR (536_T1) dataset: (a) The original tumour slice 21 (in grid), (b) Fine-tuning of misclassified blocks of the current slice, and (d) Final result of the questioned blocks 202
- 5.16 A fine-tuning result of five tumour blocks of slice 24 of MRI scan 536_88 from IBSR (536_T1) dataset: (a) The original tumour slice 24 (in grid), (b) Fine-tuning of misclassified blocks of the current slice, and (d) The final result of the questioned blocks 203
- 5.17 A fine-tuning of two wrongly tumour blocks of slice 116 of patient BRATS_HG0027 from challenge MICCAI (BRATS2012-BRATS-1) dataset: (a) The original tumour slice 116 (in grid), (b) Fine-tuning of the misclassified blocks (white blocks) of the current slice, and (d) Final result of the questioned block 204

5.18	A fine-tuning result of four tumour blocks (two separate locations) of slice 64 of patient BRATS_HG0002 from challenge MICCAI (BRATS2012-BRATS-1) dataset: (a) The original tumour slice 64 (in grid), (b) Fine-tuning of misclassified block of the current slice, and (d) Final result of the questioned block	205
5.19	A fine fine-tuning result of two tumour block of slice 95 of patient BRATS_HG0015 from challenge MICCAI (BRATS2012-BRATS-1) dataset: (a) The original tumour slice 95 (in grid), (b) Fine-tuning of misclassified blocks of the current slice, and (d) Final result of the questioned block	206
5.20	The missclassified slices of patient Normal_7 of IBSR (10Normals_T1) dataset. Red circle indicates misclassified blocks.	209
5.21	The misclassified slices of patient Normal_17 of non-tumour IBSR (10Normals_T1) dataset. Red circle indicates misclassified blocks	209
5.22	The misclassified MRI scan 536_45 of IBSR (536_T1) dataset, (a) Original MRI slice 22 with tumour inside the marked blue Square, (b) Zoomed in marked area, and (c) Misclassified blocks, where red circle indicates wrongly classified blocks and yellow circle represents the tumour area	211
5.23	The misclassified MRI scan 536_45 of IBSR (536_T1) dataset, (a) Original MRI slice 31 with tumour inside marked blue Square, (b) Zoomed in marked area, and (c) Misclassified blocks, where red circle indicates wrongly classified blocks and yellow circle represents the tumour area	212
5.24	The Jaccard coefficient and Dice coefficient	213

	similarity indices for each MRI patient in challenge MICCAI (BRATS2012-BRATS-1) dataset	
5.25	The misclassified patient BRATS_HG0004 of challenge MICCAI (BRATS2012-BRATS-1) dataset, (a) Original MRI slice 115 with tumour inside marked blue Square, (b) Enlarged marked area, and (c) Misclassified blocks, where red circle indicates wrongly classified blocks and yellow circle represents the tumour area	214
5.26	The measured Jaccard coefficient and Dice coefficient for the three distinct datasets: IBSR (10Normals_T1), IBSR (536_T1), and challenge MICCAI (BRATS2012-BRATS-1)	215
5.27	The sensitivity, specificity and accuracy of each MRI patient obtained from challenge MICCAI (BRATS2012-BRATS-1) dataset	219
5.28	The misclassification of slice 85 of the patient BRATS_HG0015 of challenge MICCAI (BRATS2012-BRATS-1) dataset, (a) Original MRI slice 85 with tumour marked with blue square, and (b) Enlarged tumour	220
5.29	The Results for the sensitivity, specificity and accuracy among the three used datasets	221
5.30	The segmentation results of the proposed method implemented on the first slice of the abnormal slices of three different scans of IBSR (536_T1) dataset	222
5.31	The segmentation results of the proposed method implemented on the middle slice of the abnormal slices of three different scans of IBSR (536_T1) dataset	223
5.32	The segmentation results of the proposed method implemented on the abnormal slices of four	

	patients of challenge MICCAI (BRATS2012-BRATS-1) dataset	225
5.33	The segmentation results of the proposed method implemented on slices with a multi-locations tumour for patient BRATS_HG0007 of challenge MICCAI (BRATS2012-BRATS-1) dataset	227
5.34	The segmentation results of the proposed method implemented on slices with a multi-locations tumour for patient BRATS_HG0026 of challenge MICCAI (BRATS2012-BRATS-1) dataset	227
5.35	Multi-locations tumours “merged” for patient BRATS_HG0007 of challenge MICCAI (BRATS2012-BRATS-1) dataset	228
5.36	The misclassification of tumour tissues of MRI scan 536_88 of IBSR (536_T1) dataset, (a) Original slice 23 with tumour (blue Square), (b) Enlarged tumour (c) Misclassified tumour pixels (red circle) – real tumour is in yellow circle	231
5.37	The misclassified tumour of patient BRATS_HG0005 in challenge MICCAI (BRATS2012-BRATS-1) dataset, (a) Original slice 71 with tumour (blue square), and (b) Magnified tumour (red circle)	233
5.38	Jaccard and Dice indices: The proposed method versus the state-of-the-art techniques for the challenge MICCAI (BRATS2012-BRAT-1) dataset	234
5.39	Sensitivity and specificity: The proposed method versus the state-of-the-art techniques for the challenge MICCAI (BRATS2012-BRAT-1) dataset	234
5.40	3D visualization of the MR scanned egg, (a) The real egg, (b) Generated by the Matlab's Meshing Point Clouds function, (c) Generated by the Proposed method	237

5.41	3D visualization of the MR scanned potato, (a) The real potato, (b) Generated by the Matlab's Meshing Point Clouds function, (c) Generated by the Proposed method.	238
5.42	The 3D visualization of brain tumour for patient BRATS_HG0011 of challenge MICCAI (BRATS2012-BRATS-1) dataset using: (a) The Meshing Point Clouds, and (b) The proposed method	240
5.43	The 3D visualization of brain tumour for patient BRATS_HG0012 of challenge MICCAI (BRATS2012-BRATS-1) dataset using: (a) The Meshing Point Clouds, and (b) The proposed method	241
5.44	The 3D visualization of brain tumour for patient BRATS_HG0007 of MICCAI (RATS2012-BRATS-1) dataset using: (a) The Meshing Point Clouds and (b) The proposed method	242
5.45	The 3D visualization of brain tumour for patient BRATS_HG0027 of MICCAI (RATS2012-BRATS-1) dataset using: (a) The Meshing Point Clouds and (b) The proposed method	243
5.46	The 3D visualization of two brain tumours for patient BRATS_HG0002 of challenge MICCAI (RATS2012-BRATS-1) dataset using: (a) Meshing Point Clouds, (b) The proposed method with 0° rotation, (c) The proposed method with 60° rotation, and (d) The proposed method with 120° rotation	245
5.47	State of the brain tumour progression viewed in 3D images produced by the Meshing Point Clouds function with IBSR (536_T1) dataset: (a) First MRI scan 536_32, (b) Second MRI scan 536_45, (c) Third MRI scan 536_47, (d) Fourth MRI scan	248

	536_68, and (e) Fifth MRI scan 536_88	
5.48	State of the brain tumour progression viewed in 3D images produced by the proposed method with IBSR(536_T1) dataset, where dark colour represents healthy tissues and light colour denotes the cancerous tissue. (a) First MRI scan 536_32, (b) Second MRI scan 536_45, (c) Third MRI scan 536_47, (d) Fourth MRI scan 536_68 and (e) Fifth MRI scan 536_88	249
5.49	Volume comparison of six irregular objects (egg, meat, carrot, cucumber, potato, and green pepper) obtained using different methods	251
5.50	The proposed method versus four standard volume measures in terms volume error rates of six irregular objects	253
5.51	Calculated tumour volumes of IBSR (536_T1) dataset: Comparison between the proposed method and the four standard measures	254
5.52	Calculated tumour volumes of challenge MICCAI (BRATS2012-BRATS-1) dataset: Comparison between the proposed method and the four standard measures	256

LIST OF ABBREVIATIONS

1D	-	One dimensional
2D	-	Two dimensional
3D	-	Three dimensional
ANFIS	-	Adaptive Network-Based Fuzzy Inference System
ANN	-	Artificial Neural Network
AR	-	Approximate Reasoning
BET	-	Brain Extraction Tool
BPNN	-	Back-Propagation Neural Networks
BRATS	-	Brain Tumour Segmentation
BSE	-	Brain Surface Extractor
CAD	-	Computer Aided Diagnostics
CF	-	Classification Forest
CHNN	-	Competitive Hopfield Neural Network
CNS	-	Central Nervous System
CSF	-	Cerebrospinal Fluid
CT	-	Computed Tomography
DT	-	Delaunay Triangulations
DWT	-	Discrete Wavelet Transform
EM	-	Expectation Maximization
FACT	-	Fully Automated Calibration Technology
FCM	-	Fuzzy c-Means
FHNN	-	Fuzzy Hopfield Neural Network
FKNN	-	Fuzzy Kohonen Neural Network
FLAIR	-	Fluid-Attenuated Inversion-Recovery

FLBPA	-	Fuzzy and Learning Back Propagation Algorithm
FN	-	False Negative
FP	-	False Positive
FP-ANN	-	Forward Back-Propagation Artificial Neural Network
FPCM	-	Fuzzy Probabilistic c-Means
GB	-	GigaByte
GBM	-	GlioBlastoma-Multiform
GC	-	Graph Cut
GHz	-	Gigahertz
GM	-	Gray Matter
GMM	-	Gaussian Mixture Models
GSFCM	-	Generalized Spatial Fuzzy c-Means
GTR	-	Gross Total Resection
HG	-	High-Grade
HH	-	High-High frequency band
HL	-	High-Low frequency band
HNN	-	Hopfield Neural Networks
HSOM	-	Hierarchical Self-Organizing Map
HWA	-	Hybrid Watershed Algorithm
IARC	-	International Agency for Research on Cancer
IBSR	-	Internet Brain Segmentation Repository
I-HF	-	Inter-Hemisphere Fissure
ISLT	-	Inverse Slantlet Transform
k-NN	-	k-Nearest Neighbors
LCC	-	Largest Connected Component
LG	-	Low-Grade
LH	-	Low-High frequency band
LL	-	Low-Low frequency band
LS-SVMs	-	Least Squares Support Vector Machines
MICCAI	-	Medical Image Computing and Computer Assisted Intervention
MLP	-	Multilayer Perceptron

MMC	-	Modified MacDonald
MRF	-	Markov Random Field
MRGM	-	Modified Region Growing Method
MRI	-	Magnetic Resonance Imaging
NN	-	Neural Network
PBT	-	Probabilistic Boosting Trees
PCA	-	Principal Component Analysis
PD	-	Proton Density
PET	-	Positron Emission Tomography
PSNR	-	Peak Signal-to-Noise Ratio
RF	-	Radio Frequency
ROI	-	Region of Interest
RW	-	Random Walker
SBRG	-	Seed-based region growing
SGLDM	-	Spatial Gray Level Dependence Method
SLT	-	Slantlet Transform
SOFM	-	Self-Organizing Feature Map
SOM	-	Self-Organizing Map
SOP	-	Standard Operating Procedure
SPECT	-	Single Photon Emission Computed Tomography
SVM	-	Support Vector Machines
TN	-	True Negative
TP	-	True Positive
UNNCK-M	-	Unsupervised Neural Network Clustering k-Means
VD	-	Volume Distribution
WAT	-	Watershed Algorithm
WCT	-	Wavelet Co-occurrence Texture features
WM	-	White Matter
WM	-	Weighted Median
WST	-	Wavelet Statistical Texture features
WT	-	Wavelet Transform

LIST OF SYMBOLS

A	-	The special area of the products of opposite sides
$a_0, a_1, b_0, b_1, c_0, c_1, d_0,$ and d_1	-	Filters-bank parameters of
a_1 and a_2	-	The tumour area in two slices
$C_1, C_2, C_3, \dots, C_8$	-	The blocks name of current mask
C_i	-	The center of current mask
$D(A,B)$	-	The coefficient value of Dice
d_1 and d_2	-	The two longest orthogonal diameters of the tumour
F	-	Set of all pixels in an MR image
f	-	First tumour slice
$H \times W$	-	Size of MR image
$I(x,y)$	-	MRI slice
$i \times i$	-	Size of SLT image (ROI)
$I_{\text{Image_test}}$	-	ROI name
$J(A,B)$	-	The coefficient value of Jaccard
$M \times N \times K$	-	M and N are the MR image size and K is the slice number
n	-	Last tumour slice
N	-	The total number of MR images in the dataset
n_i	-	The number of occurrences the tumour in the slice “i”
$P()$	-	Homogeneity predicates defined on groups of the connected pixels
P_i	-	The probability distribution (frequency of occurrence) of the tumour in the slice “i”
P_i	-	The center of preceding mask

s	-	Number of tumour slice
S_i	-	The center of succeeding mask
SLTfilter	-	SLT filter matrix
SLTfilter ^T	-	SLT transposing filter matrix
SLTimage	-	SLT image matrix
Sub ₁ , Sub ₂ , ..., Sub _n	-	Connected subsets
t	-	Slice thickness
T_1 , T_2 , and T_3	-	First, second, and third threshold
V	-	The volume of the tetrahedron
$W \times W$	-	Size of non-overlapping blocks in MRI slice
w_k	-	Is all coefficients in SLT matrix
α	-	Alpha
π	-	3.14
σ	-	Standard deviation
ε	-	Donoho universal threshold
$g_i(n)$, $f_i(n)$ and $h_i(n)$	-	SLT filters-bank
μ_i	-	The mean values
σ_1^2 and σ_2^2	-	Variances of two classes probabilities isolated by threshold “ t ”
ω_1 and ω_2	-	Two classes probabilities isolated by threshold “ t ”
ω_i	-	Class probabilities

LIST OF ALGORITHMS

ALGORITHM	TITLE	PAGE
4.1	Standard Otsu's algorithm.	113
4.2	Extraction process for Largest Connected Components (LCC).	118
4.3	Creation of a LCC binary mask	119
4.4	Cerebral tissue extraction process	121
4.5	Feature extraction process	126
4.6	Labelled tumour blocks process	135
4.7	The fine-tuning mechanism	141
4.8	Tumour slice detection	142
4.9	Calculation of parameter of $g_i(n)$ filter	147
4.10	Calculation of parameters of $f_i(n)$ and $h_i(n)$ filters	148
4.11	Calculation of coefficients of $f_i(n)$ and $h_i(n)$ filters	148
4.12	Creation of SLTfilter matrix	150
4.13	Transpose operation of SLTfilter matrix	151
4.14	Calculation process of SLTimage matrix	152
4.15	Calculation of Donoho Universal Threshold and replacing all insignificant coefficients by zeros	156
4.16	Inverse Slantlet (ISLT) composition of SLT matrix	158
4.17	Tumour Cloud Points (TCP) extraction process	162

4.18	The calculation of optimum α value algorithm.	165
4.19	Calculation of distance between two points	170
4.20	Calculation of nearest neighbour algorithm.	170
4.21	Calculation of Right Next Neighbour “RNN” algorithm	174
4.22	Construction of triangles in anticlockwise	177
4.23	Construction of Delaunay Triangulation	178
4.24	Selection of appropriate tetrahedrons	181

LIST OF APPENDICES

APPENDIX	TITLE	PAGE
A	Results of MRI slices scanning and segmentation of irregular objects.	293
B	Results of 3D visualization of irregular objects.	298
C	Results of 3D visualization of the brain tumour of patients in the challenge MICCAI (Brats2012-Brats-1) dataset.	300

CHAPTER 1

INTRODUCTION

1.1 Overview

This chapter rationalizes the urgent necessity of systematic research to detecting and segmenting the brain tumour in Magnetic Resonance Images (MRI). Brain tumour being the most common brain diseases affects and devastates many human lives (Siegel *et al.* 2012). According to the estimation of International Agency for Research on Cancer (IARC), every year over 126,000 people are diagnosed with brain tumour with a mortality rate above 97,000 (Ferlay *et al.* 2010). Despite many dedicated research efforts to overcome brain tumour related problems, higher survival rate of brain tumour patients is far from being achieved. Lately, multi-disciplinary approaches involving the knowledge of medicine, mathematics and computer science are adopted for better understanding of the disease and to discover more effective methods for cure.

MRI and Computed Tomography (CT) scans of human brain are the most common tests used to detect the presence and identify the location of brain tumour for selected specialised treatment option (Polidais 2006; Jeena and Kumar 2013). Presently, available options for brain tumour treatment include surgery, radiotherapy,

and chemotherapy. The choice for the treatment options are based on the size, shape, type, and grade of the tumour. It also depends on whether or not the tumour is exerting pressure on vital parts of the brain (Horská and Barker 2010; Tommaso 2012). Actually, the treatment options is critically decided by the factors such as the extent to which the tumour has spread to the other parts of the Central Nervous System (CNS) or body, the possible side effects on the patient relating to the treatment procedure and the overall health of the patient (Merchant *et al.* 2010).

Certainly, precise detection of the brain abnormality type is a great necessity to reduce diagnostic errors and to schedule a correct treatment plan. In this regard, Computer Aided Diagnostics (CAD) remarkably improved the detection accuracy. The CAD system not only renders an alternative opinion to support the image interpretation of the radiologist but also reduces the image reading time significantly. Brain segmentation for abnormality detection in MRI slices is the most tedious task due to its complex anatomy and problems inherent to the nature of the image (Hutchison and Mitchell 2011; Moghaddam and Soltanian-zadeh 2011; Reddy *et al.* 2012). The heterogeneous and diffuse manifestation of pathology in medical images often prohibits the employment of computational methods. Primarily, several classes for tumour types possess a variety of sizes and shapes (Prastawa *et al.* 2004; Louis *et al.* 2007). Appearance of tumour at different locations in the brain with varying image intensities is another factor that makes automated brain tumour image detection and segmentation difficult (Polidais 2006). Diffusive growth of tumours often makes their resection highly difficult. Usually, surgery is performed to achieve a Gross Total Resection (GTR) because the extent of surgical resection in turns determines the longevity of the patient (Lacroix *et al.* 2001; Stippich 2007; Merchant *et al.* 2010).

Precise determination and comparison of tumour volume on preoperative and postoperative MR images are prerequisite for the resection extent determination. The estimation of preoperative and postoperative tumour volumes are often depend on the surgeon's impression or on the measurement of its largest axis along x, y and z direction (Lacroix *et al.* 2001; Merchant *et al.* 2010). Consequently, accurate

volume calculation of tumour is not executed routinely. Definitely, the visualization of the tumour on MR images greatly diverges due to presence of varieties of tissues inside the tumour area and its diffuse expansion. Thus, the selection of different segmentation techniques is essential to differentiate the cancerous tissue from the surrounding healthy tissues. This assists to determine the correct tumour volume. Besides, the segmented tumours must be visualized distinctly to obtain their explicit shape and location in the brain.

1.2 Designations

The human brain being the central functional unit controls the entire human body parts. It is a highly specialised organ that allows human being to adapt and endure varying environmental conditions. In addition, the brain enables a human to articulate words, execute actions, bring about thoughts and feelings (Natarajan *et al.* 2012; Deepak *et al.* 2013). Under certain conditions due to mysterious reasons the brain cells grow and multiply in an uncontrolled manner. In this situation, the mechanism that controls normal cells is unable to regulate the growth of the brain cells. The abnormal mass of brain tissue is medically termed as the brain tumour. The tumour occupies the space inside the skull, intervene the regular activity of brain and enhances the brain pressure. This increased brain pressure causes some shift of the brain tissues, pushes them against the skull and responsible for the nerves damage of the other healthy brain tissues (Louis *et al.* 2007; Natarajan *et al.* 2012; Shally and Chitharanjan 2013; Salankar and Bora 2014).

Varieties of imaging modalities such as CT (Al-Kadi 2010), MRI (Wong *et al.* 2012), Single Photon Emission Computed Tomography (SPECT) (Bronnikov 2012) and Positron Emission Tomography (PET) (Wright 2010; Lartizien *et al.* 2012) are used to inspect brain tumours. Figure 1.1 shows an image slice through the human brain obtained via CT, MRI, SPECT and PET techniques to render different

information about the brain function and anatomy.

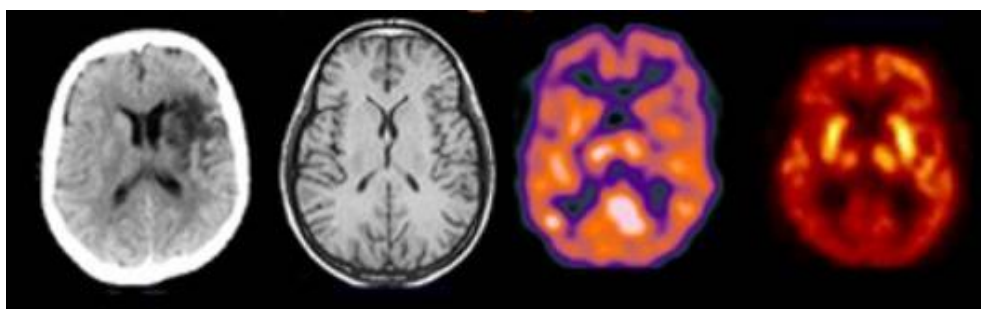


Figure 1.1 Human brain slices with different imaging modalities. From left to right: CT, MRI, SPECT and PET (Wright 2010)

Damadian invented the MRI in 1969 and first used it to investigate the human body (Damadian *et al.* 1977). Eventually, MRI became the most preferred imaging technique in radiology because it allows the visualization of internal structures in greater details. MRI reveals superior distinction among soft tissues within the body. This makes MRI suitable to generate better quality images for the cancerous tissues, brain, heart, and muscle than X-rays or CT methods (Novelline and Squire 2004; Fu *et al.* 2010; Abdullah *et al.* 2011).

Figure 1.2(a) illustrates a patient's head that is examined in a clinical diagnosis using three planes, including axial plane, coronal plane, and sagittal plane. Figure 1.2(b) to (d) depicts the brain MR images from various planes.

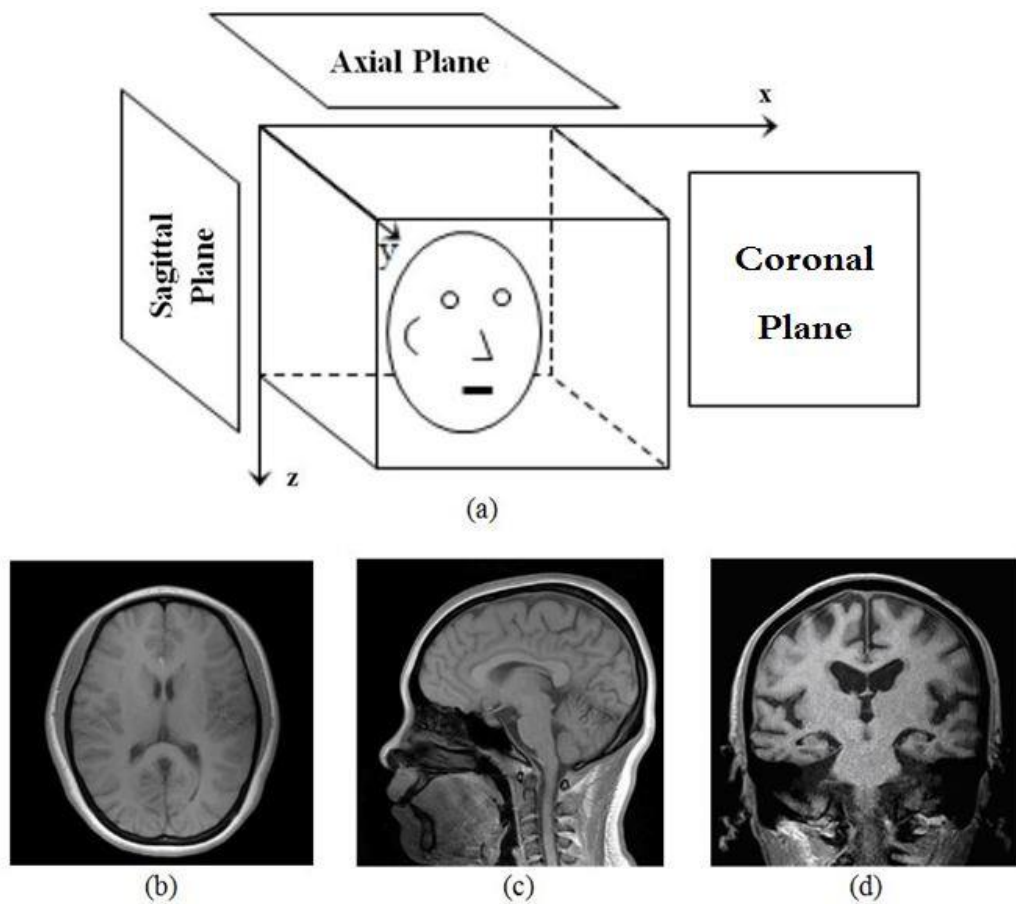


Figure 1.2 MR brain image from patient's head (a) The setup, (b) Axial plane view, (c) Sagittal plane view, and (d) Coronal plane view (Lorenzen *et al.* 2001)

MRI is represented via pixels grids with "H" rows and "W" columns. Every pixel of an MR image corresponds to a voxel (i.e. Volume element) whose value symbolizes the tissue and MR signal, respectively. The volume of a voxel depends on MR image parameters including slice thickness and pixel spacing. Normally, an MR image acquires more than one slice, which leads to an image sequence ($H \times W \times K$) with "K" slices. Figure 1.3 displays a typical MR image sequence of ($512 \times 512 \times 9$) having (5.5 mm) spacing between slices and ($0.9375 \text{ mm} \times 0.9375 \text{ mm}$) distance between each two pixels in the image slice.

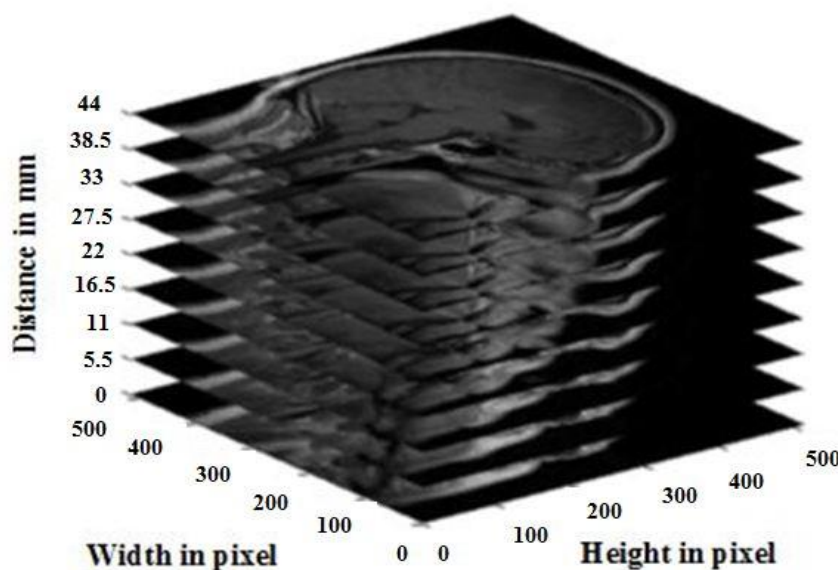


Figure 1.3 MR image sequence (Brown and Semelka 2011)

1.3 Background of Research

The medical brain images provide valuable and detailed information regarding normal and abnormal brain tissues. Currently, MR images are the most common test for diagnosing and confirming the presence of brain tumour (Horská and Barker 2010; Joshi 2010; Mehmood *et al.* 2013). Practically, brain MR images include both normal and abnormal image slices. Despite extensive research, the classification of brain MR image abnormality remains challenging (Padma and Sukanesh 2011; Elaiza *et al.* 2011a; Al-Badarneh *et al.* 2012). The reasons are due to variation of possible complex locations, size, shapes, and image intensities for different types of brain tumours (Kikinis *et al.* 1996; Xu *et al.* 2002; Veloz *et al.* 2011; Roy *et al.* 2013).

Radiologists analyse the brain MRI slices by visual inspection to detect and identify the presence of tumour or abnormal tissue (Amrutal *et al.* 2010; Salankar

and Bora 2014). These diagnoses are based on the location, shape, and image intensity of different types of brain tumours. Clinically, radiologists analyse the brain image slice by slice visually for tumour detection and identification. Such effort is labour intensive, expensive and often erroneous, especially involving a large number of image slices. Furthermore, the sensitivity of the human eye and brain to elucidate such images reduces with the increase of number of cases, particularly when only a small number of slices contain information of the affected area (Salankar and Bora 2014). Therefore, a powerful and reliable tool needs to be developed to automate the tumour localization so that precise detection and segmentation of the abnormal tissue is feasible.

Figures 1.4 and 1.5 display a normal MRI slices of patients. Figure 1.6 illustrates an abnormal MRI slice at different locations, size, shapes, and image intensities for brain tumours in the same patient.

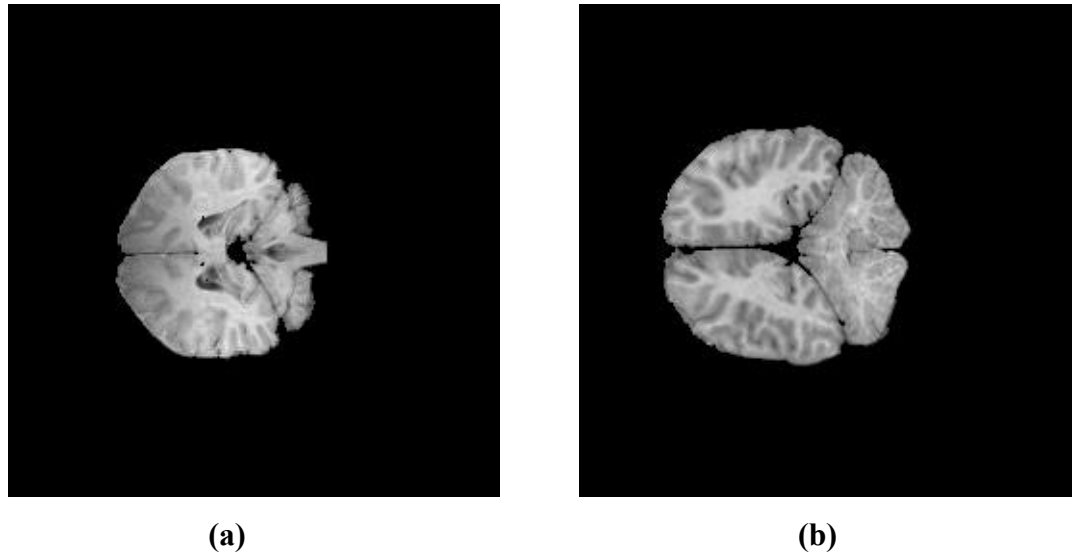


Figure 1.4 Normal MRI slices from IBSR (10Normals_T1) dataset, (a) Slice 22 of patient Normal_4, and (b) Slice 16 of patient Normal_15

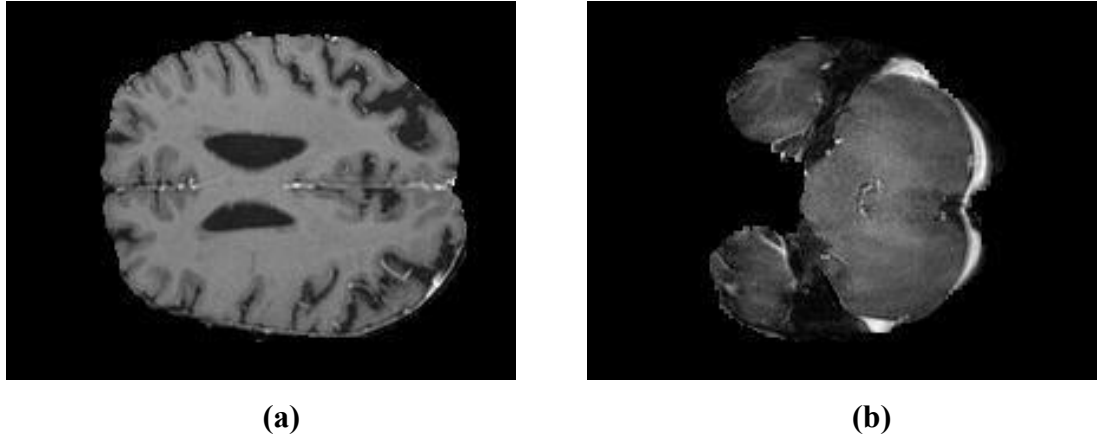


Figure 1.5 Normal MRI slices from challenge MICCAI (BRATS2012-BRATS-1) dataset, (a) Slice 119 of patient BRATS_HG0010, and (b) Slice 54 of patient BRATS_HG0008

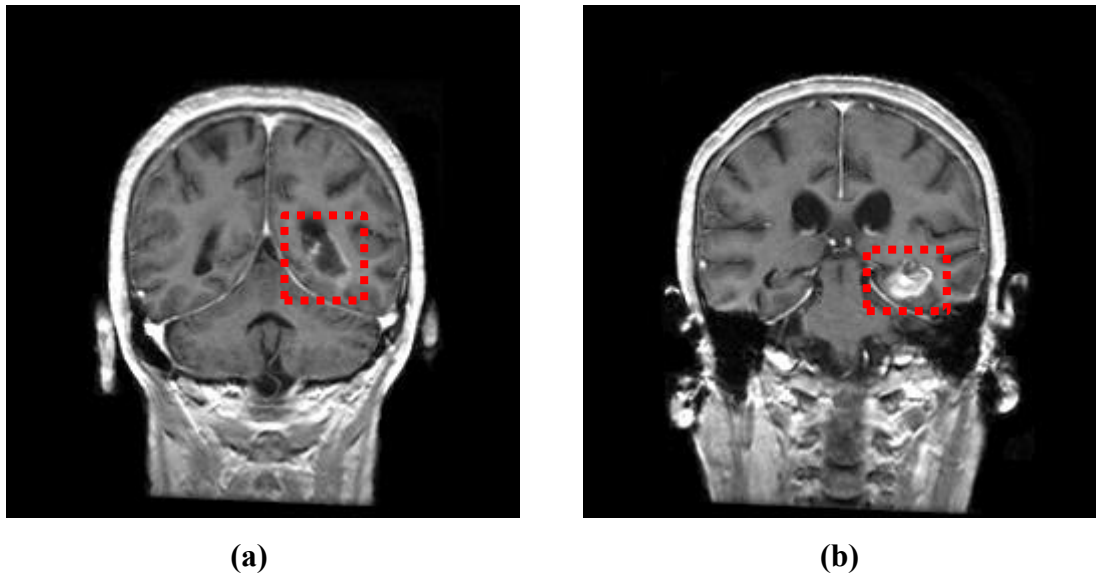


Figure 1.6 Abnormal MRI slices at different locations with varying size, shapes, and image intensities of brain tumour (red rectangle) from IBSR (536_T1) dataset of MRI scan 536_32, (a) Slice 22, and (b) Slice 26

Anatomically, MR brain images consist of non-cerebral tissues such as skull, skin, bone, muscle, eye-balls, and dura together with cerebral tissues including White Matter (WM), Gray Matter (GM), Cerebrospinal Fluid (CSF) and tumour (if

present). Separation of these types of these tissues and localization or segmentation of tumours from cerebral tissues poses a severe challenge. Present outcome is far from being satisfactory and radical improvement is necessary (Xu *et al.* 2002; Harati *et al.* 2011; Bauer *et al.* 2011; Wang *et al.* 2011; Veloz *et al.* 2011; Hamamci *et al.* 2012). Figure 1.7 illustrates the separation complexity of the healthy tissues from the cancerous one for challenge MICCAI (BRATS2012-BRATS-1) dataset reflecting the intensity homogeneity and inherent complexity.

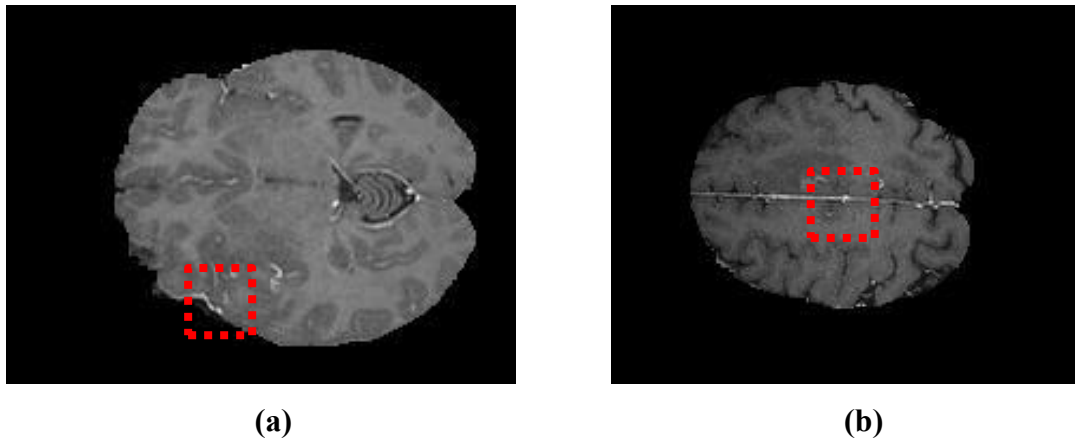


Figure 1.7 Abnormal MRI slices in the presence of tumour inside the red square in terms of intensity homogeneity from challenge MICCAI (BRATS 2012-BRATS-1) dataset, (a) Slice 85 of patient BRATS_HG0004, and (b) Slice 127 of patient BRATS_HG0007

Of late, several segmentation algorithms are extensively implemented towards diverse medical imaging modalities (Moon *et al.* 2002; Sasikala *et al.* 2006; Zacharaki *et al.* 2008; Singh *et al.* 2009; Soesanti *et al.* 2011; Mustaqeem *et al.* 2012; Gang *et al.* 2013; Sinha and Sinha 2014). These techniques used dissimilar tactics to integrate the earlier available information with automatic segmentation. The performance of such techniques is decided by both the interaction plan and automatic computation scheme. Moreover, the performance evaluation varies from application to application because different medical images enclose entirely different complex anatomical structures. Thus, these methods face difficulties in managing the peripheral concavities, fragile edges, and noises of the medical image.

Brain tumour being a well-known serious disease with absolute complexity, the diffusive growth of tumours often makes their resection highly intricate. Usually, surgery is performed to achieve a GTR because the extent of surgical resection determines the longevity of the patient (Lacroix *et al.* 2001). Indisputably, the graphical visualization is an essential part of brain tumour detection and analysis. Still, accurate brain tumour visualization remains a formidable task. It is crucial to improve the degree of resection for the abnormal tissues while preserving normal tissues (González-Navarro *et al.* 2012; Yee Lau *et al.* 2014). Methods are available to visualize the brain tumour, but the major problem with these methods is the inability to visualize the boundaries of the tumour accurately in the details. In addition, their inability to separate the healthy tissues from the unhealthy one leads to the assessment and calculation of wrong tumour volume (Lee 2009; González-Navarro *et al.* 2012; Yee Lau *et al.* 2014). Figure 1.8 shows an example of the 3D visualization method of tumour patient, where the actual border is not seen and the tumour does not reveal the difference between healthy and unhealthy tissues.

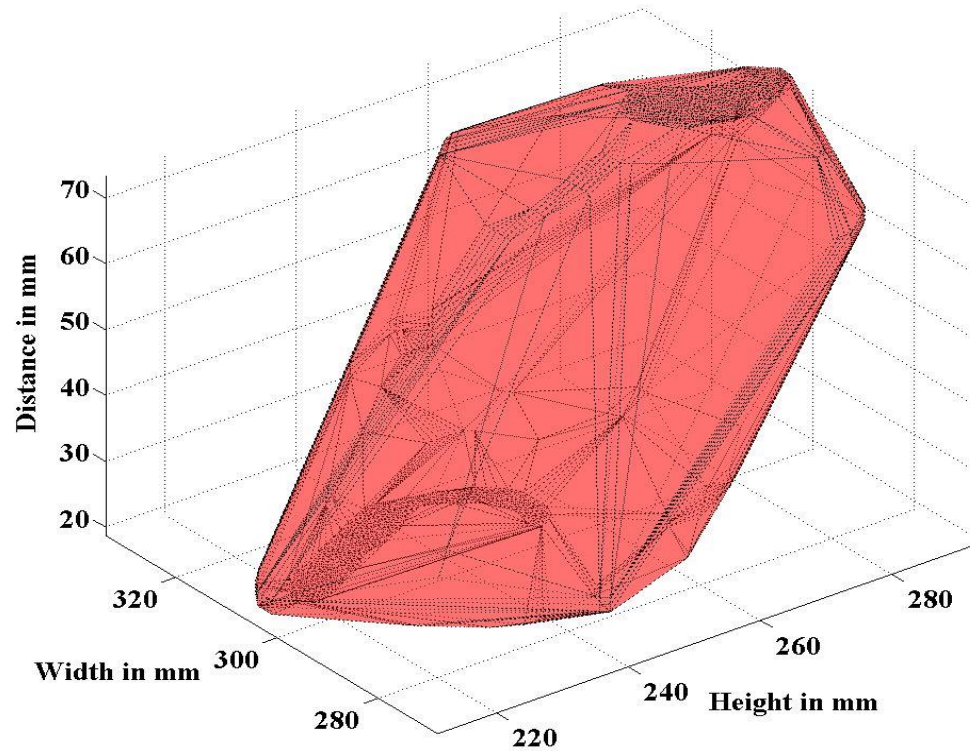


Figure 1.8 3D brain tumour visualization of MRI scan 536_32 in IBSR (536_T1) dataset using Matlab's Meshing Point Clouds function

The estimation of preoperative and postoperative tumour volumes are frequently decided by the surgeon's impression or on the measurement of its largest axis along x, y and z direction (Lacroix *et al.* 2001). Precise determination of the brain tumour extent for excised and advanced treatments requires careful calculation and systematic observation of the therapeutic effects on the tumour (Salman *et al.* 2005; Siegel *et al.* 2012; Dang *et al.* 2013). Typically, this is performed by measuring the volume of the tumour from 3D scans. Although, numerous methods for the estimation of the tumour volume are available, but the actual 3D shape of the tumour is seldom displayed. Conversely, each scientific research must evaluate and gauge their result. However, research is not yet perfected to extract the tumour from the brain and measure its volume to validate and evaluate the result given by other related method of brain tumour volume calculation. Simultaneously, there are methods to calculate the brain tumour volume manually. Some of them include Frustum Model (Shally and Chitharanjan 2013), Meshing Point Clouds (Iglesias *et al.* 2011), Trace method (Chong *et al.* 2004; Salman *et al.* 2005) and Modified MacDonald (MMC) method (Dang *et al.* 2013). However, the results obtained from these methods are not very accurate and often neglects the ground truth. Thus, it is indispensable to uncover an innovative method to gauge and validate the proposed method of tumour volume calculation.

In short, cancer is considered as the disease of the century. Despite the introduction of various methods and calculations the accurate determination of the tumour volume remains unsuccessful and many obstacles still exist that does not allow the full recovery. Moreover, overcoming the uncertainty of these methods in determining the actual volume, the brain tumour shape and the errors in drug dose calculations that lead to wrong dose (over or under) which would finally lead to jeopardizing the human life remain the future challenges. These performance limitations necessitate continued research efforts to mitigate the identified challenges.

In view of the above rationale, present thesis posed the following research questions to provide solutions to the challenges regarding abnormality detection of

MRI slices, brain tumour segmentation, 3D visualization and volume calculation of brain tumour and finally the creation of a new ground truth.

The main issues are how to detect, segment, visualise, and calculate the volume of the brain tumour in MR images with a high reliability?

The specific research questions that need to be answered are:

- i) Is it possible to determine brain abnormality accurately?
- ii) How to develop a new method to overcome the earlier limitations associated with MRI images brain tumour detection, segmentation, visualization, and volume calculation?
- iii) Can the proposed method perfectly segment the brain tumour in MRI images?
- iv) Does the new method capable to extract suitable features from the abnormal cerebral tissues which can be used to represent the brain tumour(s) in the MR images?
- v) How to determine the brain tumour(s) volume accurately using the extracted features?
- vi) Is it possible to represent and visualize the brain tumour in a 3D presentation?
- vii) How accurate and reliable the 3D visualization and computed volume of a brain tumour?
- viii) How to validate and evaluate the 3D visualization and computed volume of a brain tumour?
- ix) How to create a new ground truth for reliable assessment and implementation of the proposed methods?

1.4 Problem Statements

It is an urgent necessity to build an understanding on the brain tumour detection and subsequent analyses with systematic processing steps, including abnormality detection in MRI slices, segmentation, 3D visualization and volume calculation of brain tumour. Despite numerous available methods satisfactory results on brain tumour detection and segmentation are far from being acquired. Consequently, surgery and diagnostics remain a dispute. Different approaches are proposed for the all previous processing steps. In addition, creation of a new ground truth is mandatory. The entire brain tumour detection scheme mainly depends upon appropriate preprocessing methods in terms of accuracy and reliability. A new fully automatic detection system for brain tumour need to be introduced by taking the following views of the latest developments:

1. Clinically, detection of MRI brain slices' abnormality is painstaking, voluminous and time-consuming (Singh and Kaur 2012; Kumari 2013; Salankar and Bora 2014). This is due to two main reasons: (1) homogeneity between healthy tissues and cancerous cells, which is very difficult to distinguish even by naked eyes, let alone the machines and, (2) large number of slices involved during the examination - the figure varies whose relies on the type and severity of illnesses (Selvaraj *et al.* 2007; Abdullah *et al.* 2011; Salankar and Bora 2014). Thus, many attempts are made to automate the process. However, its performance is rather less impressive and room for improvement is still wide open. Besides, another pressing issue is to localize a tumour or cancerous cell found in the abnormal slice, automatically, which is never being of research interest thus far. Therefore, an effective solution for the above problems not only would equip the doctor with the state of the art, but would also ensure a successful implementation of subsequent procedures, including segmentation, visualization, and volume estimation of tumours in a more precise manner.
2. Definitely, the brain tumours segmentation in MRI is a challenging and difficult task (Elaiza *et al.* 2011b; Hamamci and Unal 2012; Weizman *et al.*

2014) because of the variety of possible shapes, locations, and image intensities. The pathology identification, detection of the disease and comparison between normal and abnormal tissues require assorted mathematical algorithms for features extraction, modeling, and measurement in the images. Lately, several useful segmentation algorithms were proposed (Moon *et al.* 2002; Zacharaki *et al.* 2008; Farmaki *et al.* 2010). However, due to the nature of tumour, the accuracy of the algorithms is far from satisfactory (Dass and Devi 2012; Shin 2012; Roy *et al.* 2013).

3. Another pressing issue on tumour treatment is accurate 3D visualization of the tumour. However, research interest in this area is very limited (Wu *et al.* 2008; Lee 2009; González-Navarro *et al.* 2012; Wakchaure *et al.* 2014). Unfortunately, the accuracy of their works is challengeable due to the absence of the ground truth to validate their results (Wakchaure *et al.* 2014). Also, most of the tumour shapes generated by the methods are far from satisfactory because they only provide gross shape of the tumour, let alone to distinguish between the healthy tissues and cancerous tissues (Wakchaure *et al.* 2014).
4. In the cancer treatment, the tumour volume plays a significant role in determining the recommended therapy (Shi *et al.* 1998; Nelson 2001; Dubey *et al.* 2009; Shally and Chitharanjan 2013; Mehmood *et al.* 2013). In spite of several methods for tumour volume calculation such as Meshing Point Clouds, Frustum Model, Trace Method and Modified MacDonald (MMC) the detection accuracy and reliability remains debatable due to the absence of the ground truth to validate the findings (Lau *et al.* 2005; Shally and Chitharanjan 2013). Actually, these methods fail to determine the actual size of the tumour (Shally and Chitharanjan 2013). Therefore, a precise volume calculation method is required to overcome these drawbacks.
5. For any scientific research, it is obligatory to have a ground truth so that the work can be validated (Salman *et al.* 2005; Quinn *et al.* 2013; Weizman *et al.* 2014). Regarding the 3D visualisation and volume calculation of MRI brain tumour, to the best of the author's knowledge, there is no ground truth available thus far.

1.5 Research Goal

The goal of this thesis is to develop a new MRI brain tumour detection system, which includes brain tumour detection, segmentation, 3D visualisation and volume calculation, with a higher degree of accuracy than the existing one.

1.6 Objectives of the Study

In order to achieve the above mentioned goal, the following objectives need to be accomplished:

1. To detect the abnormal slices of the MR brain images.
2. To propose a new segmentation technique using the Slantlet Transform (SLT) that can precisely localise the brain tumour from cerebral tissues.
3. To develop new techniques for 3D visualization and volume calculation of the brain tumour based on the Alpha (α) shape theory.
4. To create two ground truth s for 3D visualisation and volume calculation of MRI brain tumour, respectively.

1.7 Research Scope

This study is a synthesis of a complete process of the previous works. A novel approach to MR image classification into normal and abnormal MRI slices and segmentation of the brain tumour will be developed. Finally, it will provide a full automatic system for 3D visualization and volume calculation of human brain

tumour. Computer experiments will be performed to test the proposed system on three standard datasets. The first two datasets are obtained from the Internet Brain Segmentation Repository (IBSR) created by the Center for Morphometric Analysis, Massachusetts General Hospital (USA), named IBSR (10Normals_T1) without any brain tumour and IBSR (536_T1) with brain tumours. They are used by several researchers for brain tumour detection worldwide. The third dataset called challenge MICCAI (BRATS2012-BRATS-1). The Multimodal Brain Tumour Segmentation (BRATS) challenge was the 15th international conference on Medical Image Computing and Computer Assisted Intervention (MICCAI 2012) held in France (2012). This datasets provides a large number of brain tumour MRI scans in which the brain tumour regions have been manually delineated.

This study will mainly focus on T1-weighted High-Grade (HG) brain tumour in three planes (axial, coronal, and sagittal plane) for MR image segmentation, 3D visualization and volume calculation of elevated category. However, the Low-Grade (LG) tumour and tumour classification either benign or malignant are beyond the scope of the present thesis. In addition, another MRI pulse sequences such as T2-weighted, PD-weighted (Proton Density), and Fluid-Attenuated Inversion-Recovery (FLAIR) are not within the scope.

1.8 Significance of the Study

The aforesaid diagnosis errors developed, the reason to form the foundation for the work presented here. It is strongly believed that complete automatic brain tumour detection system can improve both the false positive and the false negative diagnosis rates. The motivation of conducting this PhD study is to propose state-of-the-art, optimized and innovative techniques for the brain tumour detection. Proposed techniques should be capable to provide promising performance in an undesirable situation such as separating the MRI slices into normal and abnormal,

precise segmentation for the brain tumour by reducing segmentation error, resolve problems associated with tumour volume calculation, and visualize the brain tumour in 3D shape, and give a new way to create a new ground truth. In light of the above mentioned issues, the results of this research will contribute to what is currently known about brain tumour detection systems. Nonetheless, the significance of this study is not only limited to knowledge enrichment, but also to the development of a new method for future implementation and brain tumour diagnosis and cure.

1.9 Thesis Outline

This thesis is organized as follows. The rest of the chapters begin with a brief description highlighting the aims of each chapter and ends with a short summary. Each chapter is developed to be self-contained, but there exists cohesion among the chapters in order to ensure the free flow of presentation and understanding of the thesis content. It should also be borne in mind that mathematical notations and definitions are introduced at various points to render a consistency and better understanding of the presentation.

Chapter 2 provides an in-depth overview of relevant literatures on MR images of brain tumour detection, segmentation, 3D visualization, and volume calculation. It is emphasised that the brain tumour in MR images is still an emerging research area with very little literatures. Subsequently, a thorough discussion is provided on various approaches used so far in the brain MR image segmentation. The limitations of the existing methods and the need to develop a new method for detecting abnormal MRI slices, segmentation, visualization and volume calculation of brain tumour problems are underscored.

Chapter 3 presents a clear roadmap of this study to guide the reader for quick grasp of the detailed research framework. The advantages of using the popular dataset in the newly developed methods are emphasized. The layout of the entire research framework, strategies, and procedures are highlighted.

Chapter 4 discusses the proposed methods in details. It covers the cerebral tissue extraction, slice abnormality detection, segmentation, 3D visualisation and volume calculation of the MRI brain tumour.

Chapter 5 provides the experimental results, detailed analyses, and discussions. It explains the qualitative and quantitative measurements that are carried out for the performance evaluations and implementation of the method for every single phase such as detection of the MRI slices abnormal, segmentation of brain tumour, brain tumour 3D visualization and volume calculation. The qualitative measurements are based on visual human inspections, while the quantitative measurements are performed using standard approaches. In addition, every process is benchmarked against the best and up-to-date techniques for segmentation and volume calculation found in the literature.

Chapter 6 concludes by emphasizing the major contributions, significant findings, and recommended future directions of the present thesis.

REFERENCES

- Abdullah, H. N., and Ali, S. A., (2010). Implementation of 8-Point Slantlet Transform Based Polynomial Cancellation Coding-OFDM System Using FPGA. *7th International Multi-Conference on Systems, Signals and Devices*, pp.1–6.
- Abdullah, N., Ngah, U. K., and Aziz, S. A., (2011). Image Classification of Brain MRI Using Support Vector Machine. *Imaging Systems and Techniques (IST), IEEE International Conference*, pp. 242–247.
- Aboutanos, G. B., Nikanne, J., Watkins, N., and Dawant, B. M., (1999). Model Creation and Deformation for the Automatic Segmentation of the Brain in MR Images. *Biomedical Engineering, IEEE Transactions*, vol.46, no.11, pp.1346–1356.
- Adams, R., and Bischof, L., (1994). Seeded Region Growing. *Pattern Analysis and Machine Intelligence, IEEE Transactions*, vol.16, no.6, pp.641–647.
- Al-Badarneh, A., Najadat, H., and Alraziqi, A. M., (2012). A Classifier to Detect Tumor Disease in MRI Brain Images. *Advances in Social Networks Analysis and Mining (ASONAM), IEEE/ACM International Conference*.pp. 784–787.
- Alia, O. M., Mandava, R., and Aziz, M. E., (2011). A Hybrid Harmony Search Algorithm for MRI Brain Segmentation. *Evolutionary Intelligence*, vol.4, no.1, pp.31–49.
- Al-Kadi, O. S., (2010). Assessment of Texture Measures Susceptibility to Noise in Conventional and Contrast Enhanced Computed Tomography Lung Tumour Images. *Computerized Medical Imaging and Graphics*, vol.34, no.6, pp.494–503.
- Altman, D. G., and Bland, J. M., (1994). Diagnostic Tests 1 Sensitivity and Specificity. *BMJ: British Medical Journal*, vol.308, pp.1552–1553.

- Amrutal, A., Gole, A., and Karunakar, Y., (2010). A Systematic Algorithm for 3-D Reconstruction of MRI based Brain Tumors using Morphological Operators and Bicubic Interpolation. *Computer Technology and Development (ICCTD), 2nd International Conference on. IEEE.* pp.305–309.
- Angelini, E. D., Delon, J., Bah, A. B., Capelle, L., and Mandonnet, E., (2012). Differential MRI Analysis for Quantification of Low Grade Glioma Growth. *Medical Image Analysis*, vol.16, no.1, pp.114–126.
- Antonie, L., (2008). Automated Segmentation and Classification of Brain Magnetic Resonance Imaging. *C615 Project*, pp.1-15.
- Ariffanan, M. and Basri, M., (2008). Medical Image Classification and Symptoms Detection Using Neuro Fuzzy. *Universiti Teknologi Malaysia, Faculty of Electrical Engineering, Malaysia.*
- Aurdal, L., (2006). *Image Segmentation Beyond Thresholding*. First Edition. Norsk Regnesentral.
- Avison, J., (1989). *The World of Physics*. Second Edition, Thomas Nelson and Sons.
- Badran, E. F., Mahmoud, E. G., and Hamdy, N., (2010). An Algorithm for Detecting Brain Tumors in MRI Images. *The International Conference on Computer Engineering and Systems*. IEEE, pp. 368–373.
- Baillard, C., Hellier, P., and Barillot, C., (2001). Segmentation of Brain 3D MR Images Using Level Sets and Dense Registration. *Medical Image Analysis*, vol.5, pp.185–194.
- Balafar, M. A., Ramli, A. R., Mashohor, S., and Farzan, A., (2010). Compare Different Spatial Based Fuzzy-C_{mean} (FCM) Extensions for MRI Image Segmentation. *Computer and Automation Engineering (ICCAE), The 2nd International Conference. IEEE.* pp. 609–611.
- Balafar, M. A., (2012). Gaussian Mixture Model Based Segmentation Methods for Brain MRI Images. *Artificial Intelligence Review*, pp.429–439.
- Balafar, M. A., Ramli, A., and Mashohor, S., (2011). Brain Magnetic Resonance Image Segmentation Using Novel Improvement for Expectation Maximizing. *Neurosciences*, vol.16, no.3, pp.242–247.
- Bauer, S., Fejes, T., Slotboom, J., Wiest, R., Nolte, L. P., and Reyes, M., (2012). Segmentation of Brain Tumor Images Based on Integrated Hierarchical Classification and Regularization. *Process MICCAI-BRATS (Multimodal Brain Tumor Segmentation Challenge)*, pp.10–13.

- Bauer, S., Nolte, L. P., and Reyes, M., (2011). Fully Automatic Segmentation of Brain Tumor Images Using Support Vector Machine Classification in Combination With Hierarchical Conditional Random Field Regularization. *Medical Image Computing and Computer-Assisted Intervention : MICCAI*. pp. 354–361.
- Berg, M. D., Cheong, O., Kreveld, M. V., and Overmars, M., (2000). *Computational Geometry - Algorithms and Applications*. Second Edition, Springer.
- De B., Mark, C., Otfried, V. K., Marc, O., (2008). Delaunay Triangulations. *Algorithms and Applications*. pp.191–218.
- Bermel, R. A., Sharma, J., Tjoa, C.W., Puli, S. R., and Bakshi, R., (2003). A Semiautomated Measure of Whole-Brain Atrophy in Multiple Sclerosis. *Journal of the Neurological Sciences*, vol.208, no.1-2, pp.57–65.
- Bezdek, J. C., Ehrlich, R., and Full, W., (1984). FCM: The Fuzzy c-Means Clustering Algorithm. *Computers and Geosciences*, vol.10, no.2, pp.191–203.
- Birkbeck, N., Cobzas, D., Jagersand, M., Murtha, A., and Kesztyues, T., (2009). An Interactive Graph Cut Method for Brain Tumor Segmentation. *Workshop on Applications of Computer Vision (WACV)*, pp.1–7.
- Blanton, R. E., Levitt, J. G., Peterson, J. R., Fadale, D., Sporty, M. L., and Lee, M., (2004). Gender Differences in the Left Inferior Frontal Gyrus in Normal Children. *NeuroImage*, vol.22, no.2, pp.626–636.
- Boesen, K., Rehm, K., Schaper, K., Stoltzner, S., Woods, R., Lüders, E., and Rottenberg, D., (2004). Quantitative Comparison of Four Brain Extraction Algorithms. *NeuroImage*, vol.22, no.3, pp.1255–1261.
- Bourouis, S., and Hamrouni, K., (2010). 3D Segmentation of MRI Brain Using Level Set and Unsupervised Classification. *International Journal of Image and Graphics*, vol.10, no.1, pp.135–154.
- Bronnikov, A. V., (2012). SPECT Imaging With Resolution Recovery. *IEEE Transactions on Nuclear Science*, vol.59, no.4, pp.1458–1464.
- Brown, M. A., and Semelka, R. C., (2011). *MRI Basic Principles and Applications*, Fourth Edition, Hoboken, New Jersey: John Wiley and Sons, Inc.
- Buxton, R. B., (2009). *Introdcutin to Functional Magnetic Resonance Imaging: Principles and Techniques*. Second Edition., New York - USA: Cambridge University Press.

- Cawley, G. C., and Talbot, N. L. C., (2004). Fast Exact Leave-One-Out Cross-Validation of Sparse Least-Squares Support Vector Machines. *Neural Networks : the Official Journal of the International Neural Network Society*, vol.17, no.10, pp.1467–1475.
- Chaplot, S., Patnaik, L. M., and Jagannathan, N. R., (2006). Classification of Magnetic Resonance Brain Images Using Wavelets as Input to Support Vector Machine and Neural Network. *Biomedical Signal Processing and Control*, vol.1, no.1, pp.86–92.
- Chen, S., (2004). Chaotic Spread Spectrum Watermarking for Remote Sensing Images. *Journal of Electronic Imaging*, vol.13, no.1, pp.146–165.
- Cheng, H. L., and Shi, X., (2009). Quality Mesh Generation for Molecular Skin Surfaces Using Restricted Union of Balls. *Computational Geometry*, vol.42, no.3, pp.196–206.
- Cheng, K. S., Lin, J. S., and Mao, C. W., (1996). The Application of Competitive Hopfield Neural Network to Medical Image Segmentation. *IEEE Transactions on Medical Imaging*, vol.15, no.4, pp.560–570.
- Chong, V. F. H., Zhou, J.-Y., Khoo, J. B., Huang, J., and Lim, T. K., (2004). Tongue Carcinoma: Tumor Volume Measurement. *International Journal of Radiation Oncology Biology Physics*, vol.59, no.1, pp.59–66.
- Christ, M. J., Sasikumar, K., and Parwathy, R. M. S., (2009). Application of Bayesian Method in Medical Image Segmentation. *International Journal of Computing Science and Communication Technologies*, vol.2, no.1, pp.353–355.
- Clark, M. C., Hall, L., Goldgof, D. B., Clarke, L. P., Velthuizen, R. P., and Silbiger, M.S., (1994). MRI Seamentation Usina Fuzzy Clustering TechnGues. *Engineering in Medicine and Biology Magazine, IEEE*, vol.13, no.5, pp.730–742.
- Cueto, E., Doblare, M., and Gracia, L., (2000). Imposing Essential Boundary Conditions in the Natural Element Method by Means of Density-Scaled Alpha-Shapes. *International Journal for Numerical Methods in Engineering*, vol.49, no.4, pp.519–546.
- Damadian, R., Goldsmith, M., and Minkoff, L., (1977). NMR In Cancer: XVI. FONAR Image of the Live Human Body. *Physiological Chemistry and Physics*, vol.9, no.1, pp.97–100.

- Dang, M., Modi, J., Roberts, M., Chan, C., and Mitchell, J. R., (2013). Validation Study of a Fast, Accurate, and Precise Brain Tumor Volume Measurement. *Computer Methods and Programs in Biomedicine*, vol.111, no.2, pp.480–487.
- Dass, R. and Devi, S., (2012). Image Segmentation Techniques. *International Journal of Electronics & Communication Technology (IJECT)*, vol.3, no.1, pp.66–70.
- De-Alarcón, P. A., Pascual-Montano, A., Gupta, A., and Carazo, J. M., (2002). Modeling Shape and Topology of Low-Resolution Density Maps of Biological Macromolecules. *Biophysical Journal*, vol.83, no.2, pp.619–632.
- DeCarli, Charles, Maisog, J., Murphy, D. G., Teichberg, D., Rapoport, S.I., and Horwitz, B., (1992). Method for Quantification of Brain, Ventricular, and Subarachnoid CSF Volumes from MR Images. *Journal of Computer Assisted Tomography*, vol.16, no.2, pp.274–284.
- Deepak, K. S., Gokul, K., Hinduja, R., and Rajkumar, S., (2013). An Efficient Approach To Predict Tumor In 2D Brain Image Using Classification Techniques. *Information Communication and Embedded Systems (ICICES), International Conference. IEEE*. pp. 559–564.
- Dempsey, M. F., Condon, B. R., and Hadley, D. M., 2005. Measurement of Tumor “Size” in Recurrent Malignant Glioma : 1D, 2D, or 3D ?. *American Journal of Neuroradiology*, vol.26, no.4, pp.770–776.
- Dice, L. R., (1945). Measures of the Amount of Ecologic Association Between Species. *Ecology*, vol.26, no.(3), pp.297–302.
- Dominik, W. et al., (2008). *How Does MRI Work?: An Introduction to the Physics and Function of Magnetic Resonance Imaging*. Second Edition. Springer-Verlag Berlin Heidelberg.
- Donoho, D. L., (1995). De-Noising by Soft-Thresholding. *IEEE Transactions on Information Theory*, vol.41, no.3, pp.613–627.
- Donoho, D. L., and Johnstone, I. M., (1994). Ideal Denoising in an Orthonormal Basis Chosen from a Library of Bases. *Comptes Rendus de l’Academie des Sciences-Serie I-Mathematique*, vol.319, no.12, pp.1317–1322.
- Dou, W., Ruan, S., Chen, Y., Bloyet, D., and Constans, J. M., (2007). A Framework of Fuzzy Information Fusion for the Segmentation of Brain Tumor Tissues on MR Images. *Image and Vision Computing*, vol.25, no.2, pp.164–171.
- Dubey, R. B., Hanmandlu, M., and Gupta, S. K., (2009). Region Growing for MRI

- Brain Tumor Volume Analysis. *Indian Journal of Science and Technology*, vol.2, no.9, pp.26–31.
- Dubey, R. B., Hanmandlu, M., and Gupta, S. K., (2009). Semi-Automatic Segmentation of MRI Brain Tumor. *ICGST-GVIP Journal*, vol.9, no.4, pp.1–8.
- Duncan, J. S., Member, S., and Ayache, N., (2000). Medical Image Analysis : Progress Over Two Decades and the Challenges Ahead. *Pattern Analysis and Machine Intelligence, IEEE Transactions*, vol.22, no.1, pp.85–106.
- Dunn, J.C., (1973). A Fuzzy Relative of the ISODATA Process and Its Use in Detecting Compact Well-Separated Clusters. *Cybernetics and Systems*, vol.3, no.3, pp.32–57.
- Edelsbrunner, H., (2010). Alpha Shapes - A Survey. *Tessellations in the Sciences*, pp.1–25.
- Edelsbrunner, H., Facello, M., and Liang, J., (1998). On the Definition and the Construction of Pockets in Macromolecules. *Discrete Applied Mathematics*, vol.88, no.1, pp.83–102.
- Edelsbrunner, H., Kirkpatrick, D., and Seidel, R., (1983). On the Shape of a Set of Points in the Plane. *IEEE Transactions on Information Theory*, vol.29, no.4, pp.551–559.
- Eggert, L. D., Sommer, J., Jansen, A., Kircher, T., and Konrad, C., (2012). Accuracy and Reliability of Automated Gray Matter Segmentation Pathways on Real and Simulated Structural Magnetic Resonance Images of the Human Brain. *PloS one*, vol.7, no.9, pp.1–9.
- Egmont-Petersen, M., Deridder, D., and Handels, H., (2002). Image Processing With Neural Networks-A Review. *Pattern Recognition*, vol.35, no.10, pp.2279–2301.
- Elaiza, N., Khalid, A., Ibrahim, S., and Manaf, M., (2011a). Brain Abnormalities Segmentation Performances Contrasting : Adaptive Network-Based Fuzzy Inference System (ANFIS) vs K-Nearest Neighbors (k-NN) vs Fuzzy c-Means (FCM). *15th World Scientific and Engineering Academy and Society (WSEAS) International Conference on Computers*, pp.15–17.
- Elaiza, N., Khalid, A., Ibrahim, S., and Manaf, M., (2011b). Comparative Study of Adaptive Network-Based Fuzzy Inference System (ANFIS), k-Nearest for Brain Abnormalities Segmentation. *International Journal of Computers*,

- vol.5, no.4, pp.513–524.
- El-Dahshan, E. S. A., Hosny, T., and Salem, A. B. M., (2010). Hybrid Intelligent Techniques for MRI Brain Images Classification. *Digital Signal Processing*, vol.20, no.2, pp.433–441.
- Erasmus, L. J., Hurter, D., Naudé, M., Kritzinger, H. G., and Acho, S., (2004). Review Article: A Short Overview of MRI Artefacts. *SA Journal of Radiology*, vol.8, no.2, pp.13–17.
- Farmaki, C., Marias, K., Sakkalis, V., and Graf, N., (2010). Spatially Adaptive Active Contours: A Semi-Automatic Tumor Segmentation Framework. *International Journal of Computer Assisted Radiology and Surgery*, vol.5, no.4, pp.369–384.
- Fazel Zarandi, M. H., Zarinbal, M., and Izadi, M., (2011). Systematic Image Processing for Diagnosing Brain Tumors: A Type-II Fuzzy Expert System Approach. *Applied Soft Computing*, vol.11, no.1, pp.285–294.
- Fennema-Notestine, C., Ozyurt, I. B., Clark, C. P., Morris, S., Bischoff-Grethe, A., Bondi, M. W., Jernigan, T. L., Fischl, B., Segonne, F., Shattuck, D. W., Leahy, Richard M., Rex, D. E., Toga, A. W., Zou, K. H., BIRN, M., and Brown, G., (2006). Quantitative Evaluation of Automated Skull-Stripping Methods Applied to Contemporary and Legacy Images: Effects of Diagnosis, Bias Correction, and Slice Location. *Human Brain Mapping*, vol.27, no.2, pp.99–113.
- Ferlay, J. Shin, H. R., Bray, F., Forman, D., Mathers, C., and Parkin, D. M., (2010). GLOBOCAN 2008, Cancer Incidence and Mortality Worldwide: IARC CancerBase. *Lyon, France: International Agency for Research on Cancer*, pp.101-109.
- Foltz, W. D., and Jaffray, D. A., (2004). Principles of Magnetic Resonance Imaging. *Revista mexicana de fisica*, vol. 50, no.3, pp.272–286.
- Fu, J. C., Chen, C. C., Chai, J. W., Wong, S. T. C., and Li, I. C., (2010). Image Segmentation by EM-Based Adaptive Pulse Coupled Neural Networks in Brain Magnetic Resonance Imaging. *Computerized Medical Imaging and Graphics : the Official Journal of the Computerized Medical Imaging Society*, vol.34, no.4, pp.308–320.
- Gang, Z., Dan, Z., Ying, H., Xiaobo, H., Yong, Z., Weishi, L., and Yang, Z., (2013). An Unsupervised Method for Brain MRI Segmentation. *International Journal*

- of Emerging Technology and Advanced Engineering*, vol.3, no.10, pp.8–13.
- Geremia, E., Menze, B. H., and Ayache, N., (2012). Spatial Decision Forests for Glioma Segmentation in Multi-Channel MR Images. *Process MICCAI-BRATS (Multimodal Brain Tumor Segmentation Challenge)*, pp.14–18.
- Ghesu, F. C., Wels, M., Jerebko, A., Michael, S., Hornegger, J., and Kelm, B. M., (2014). Integrated Spatio-Temporal Segmentation Of Longitudinal Brain Tumor Imaging Studies. *Medical Computer Vision. Large Data in Medical Imaging, Springer International Publishing*, pp.74–83.
- Giesen, J., Cazals, F., Pauly, M., and Zomorodian, A., (2006). The Conformal Alpha Shape Filtration. *The Visual Computer*, vol.22, no.8, pp.531–540.
- Ginneken, V. B., Frangi, A. F., Staal, J. J., Romeny, Bart M. T. H., and Viergever, M. A., (2002). Active Shape Model Segmentation With Optimal Features. *Medical Imaging, IEEE Transactions*, vol.21, no.8, pp.924–933.
- Gonzalez, R. C., Woods, R. E., and Hall, P., (2002). *Digital Image Processing*. Second Edition. New Jersey: Tom Robbins.
- González-Navarro, Fernando, F., and Belanche-Muñoz, L. A., (2012). Feature Selection for the Prediction and Visualization of Brain Tumor Types Using Proton Magnetic Resonance Spectroscopy Data. *Computational Intelligence Methods for Bioinformatics and Biostatistics. Springer Berlin Heidelberg*, pp.83–97.
- Gordillo, N., Montseny, E., Sobrevilla, P., and Member, S., (2010). A New Fuzzy Approach to Brain Tumor Segmentation. *Fuzzy Systems (FUZZ), IEEE International Conference*, pp. 1–8.
- Grau, V., Mewes, A. U. J., Alcañiz, M., Kikinis, R., and Warfield, S. K., (2004). Improved Watershed Transform for Medical Image Segmentation Using Prior Information. *IEEE Transactions on Medical Imaging*, vol.23, no.4, pp.447–458.
- Guo, B., Menon, J., and Willette, B., (1997). Surface Reconstruction Using Alpha Shapes. *Computer Graphics Forum*, vol.16, no.4, pp.177–190.
- Hahn, H. K., and Peitgen, H., (2000). The Skull Stripping Problem in MRI Solved by a Single 3D Watershed Transform. *Medical Image Computing and Computer-Assisted Intervention–MICCAI 2000. Springer Berlin Heidelberg*, pp.134–143.
- Hamamci, A., Kucuk, N., Karaman, K., Engin, K., and Unal, G., (2012). Tumor-Cut:

- Segmentation of Brain Tumors on Contrast Enhanced MR Images for Radiosurgery Applications. *IEEE Transactions on Medical Imaging*, vol.31, no.3, pp.790–804.
- Hamamci, A., and Unal, G., (2012). Multimodal Brain Tumor Segmentation Using The “Tumor-Cut” Method on The BraTS Dataset. *Process MICCAI-BRATS (Multimodal Brain Tumor Segmentation Challenge)*, pp.19–23.
- Haralick, R. M., and Shapiro, L. G., (1985). Image Segmentation Techniques. *International Society for Optics and Photonics*, pp.2–9.
- Harati, V., Khayati, R., and Farzan, A., (2011). Fully Automated Tumor Segmentation Based on Improved Fuzzy Connectedness Algorithm in Brain MR Images. *Computers in Biology and Medicine*, vol.41, no.7, pp.483–492.
- Hatano, K., Sekiya, Y., Araki, H., Sakai, M., Togawa, T., Narita, Y., Akiyama, Y., Kimura, S., and Ito, H., (1999). Evaluation of the Therapeutic Effect of Radiotherapy on Cervical Cancer Using Magnetic Resonance Imaging. *International Journal of Radiation Oncology Biology Physics*, vol.45, no.3, pp.639–644.
- Hemanth, D. J., Vijila, C. K. S., and Anitha, J., (2010). Application of Neuro-Fuzzy Model for MR Brain Tumor Image Classification. *Biomedical Soft Computing and Human Sciences*, vol.16, no.1, pp.95–102.
- Hojjatoleslami, S. A., and Kruggel, F., (1999). Segmentation of White Matter Lesions from Volumetric MR Images. *Medical Image Computing and Computer-Assisted Intervention–MICCAI’99*, pp.52–62.
- Van Horn, J. D., Ellmore, T. M., Esposito, G., and Berman, K. F., (1998). Mapping Voxel-Based Statistical Power on Parametric Images. *NeuroImage*, vol.7, no.2, pp.97–107.
- Horsfield, M. A., Rovaris, M., Rocca, M. A., Rossi, P., Benedict, R. H. B., Filippi, M., and Bakshi, R., (2003). Whole-Brain Atrophy in Multiple Sclerosis Measured By Two Segmentation Processes From Various MRI Sequences. *Journal of the Neurological Sciences*, vol.216, no.1, pp.169–177.
- Horská, A., and Barker, P. B., (2010). Imaging of Brain Tumors: MR Spectroscopy and Metabolic Imaging. *Neuroimaging Clinics of North America*, vol.20, no.3, pp.293–310.
- Hricak, H., Quivey, J. M., Campos, Z., Gildengorin, V., Hindmarsh, T., Bis, K. G., Stern, J. L., Phillips, T. L., (1993). Carcinoma of the Cervix: Predictive

- Value of Clinical and Magnetic Resonance (MR) Imaging Assessment of Prognostic Factors. *International Journal of Radiation Oncology Biology Physics*, vol.27, no.4, pp.791–801.
- Hricak, H., Lacey, C. G., Sandles, L. G., Chang, Y. C., Winkler, M. L., and Stern, J. L., (1988). Invasive Cervical Carcinoma: Comparison of MR Imaging and Surgical Findings. *Radiology*, vol.166, no.3, pp.623–631.
- Hsieh, T. M., Liu, Y. M. Liao, C. C., Xiao, F., Chiang, I. J., and Wong, J. M., (2011). Automatic Segmentation of Meningioma from Non-Contrasted Brain MRI Integrating Fuzzy Clustering and Region Growing. *BMC Medical Informatics and Decision Making*, vol.11, no.1, p.54-66.
- Huang, A., Abugharbieh, R., Tam, R., and Traboulsee, A., (2006). MRI Brain Extraction with Combined Expectation Maximization and Geodesic Active Contours. *Signal Processing and Information Technology, IEEE International Symposium*, pp.107–111.
- Huh, S., Ketter, T. A., Sohn, K. H., and Lee, C., (2002). Automated Cerebrum Segmentation From Three-Dimensional Sagittal Brain MR Images. *Computers in Biology and Medicine*, vol.32, no.5, pp.311–328.
- Hutchison, D., and Mitchell, J. C., (2011). *Machine Learning in Medical Imaging*. First Edition. Springer-Verlag Berlin Heidelberg.
- Hwang, J., Han, Y., and Park, H., 2011. Skull-Stripping Method for Brain MRI Using a 3D Level Set with a Speedup Operator. *Journal of Magnetic Resonance Imaging*, vol.34, no.2, pp.445–456.
- Ibrahim, S., Khalid, N. E. A., and Manaf, M., (2010). Seed-Based Region Growing (SBRG) vs Adaptive Network-Based Inference System (ANFIS) vs Fuzzy c-Means (FCM): Brain Abnormalities Segmentation. *International Journal of Electrical and Computer Engineering*, vol.02, no.44, pp.425–435.
- Iftekharuddin, K. M., Zheng, J., Islam, M. A., and Ogg, R. J., (2009). Fractal-Based Brain Tumor Detection in Multimodal MRI. *Applied Mathematics and Computation*, vol.207, no.1, pp.23–41.
- Igarashi, Y., and Suzuki, H., (2011). Cover Geometry Design Using Multiple Convex Hulls. *Seimitsu Kogaku Kaishi/Journal of the Japan Society for Precision Engineering*, vol.77, no.11, pp.1033–1038.
- Iglesias, J. E., Liu, C.-Y., Thompson, P. M., and Tu, Z., (2011). Robust Brain Extraction Across Datasets and Comparison With Publicly Available

- Methods. *Medical Imaging, IEEE Transactions*, vol.30, no.9, pp.1617–1634.
- Improved, A., Gradient, C., and Svm, L. S., (2005). An Improved Conjugate Gradient Scheme to the Slution of Least Squares SVM. *Neural Networks, IEEE Transactions*, vol.16, no.2, pp.498–501.
- Jabbar, N.I., and Mehrotra, M., (2008). Application of Fuzzy Neural Network for Image Tumor Description. *Proceedings of World Academy of Science*, vol.1, pp.575–577.
- Jaccard, P., (1912). The Distribution of the Flora in the Alphine Zone. *The New Phytologist*, vol.2, pp.37–50.
- Jaffar, M. A., Ain, Q., and Choi, T. S., (2012). Tumor Detection From Enhanced Magnetic Resonance Imaging Using Fuzzy Curvelet. *Microscopy Research and Technique*, vol.75, no.4, pp.499–504.
- Jahne, B., (2005). *Digital Image Processing*. Sixth Edition., Springer-Verlag Berlin, Germany.
- Jain, R., Kasturi, R., and Schunck, B. G., (1995). *Machine Vision*. First Edition. New York: McGraw-Hill.
- Jain, S., (2013). Brain Cancer Classification Using GLCM Based Feature Extraction in Artificial Neural Network. *International Journal of Computer Science and Engineering Technology*, vol.4, no.7, pp.966–970.
- Jauhiainen, Tomm, Järvinen, V. M., Hekali, P. E., Poutanen, V.-P., Penttilä, A., and Kupari, M., (1998). MR Gradient Echo Volumetric Analysis of Human Cardiac Casts: Focus on the Right Ventricle. *Journal of Computer Assisted Tomography*, vol.22, no.6, pp.899–903.
- Jeena, R. S., and Kumar, S., (2013). A Comparative Analysis of MRI and CT Brain Images for Stroke Diagnosis. *Emerging Research Areas and 2013 International Conference on Microelectronics, Communications and Renewable Energy (AICERA/ICMiCR), IEEE*. pp. 1–5.
- Jernigan, T. L., Archibald, S. L., Fennema-Notestine, C., Gamst, A. C., Stout, J. C., Bonner, J., and Hesselink, J. R., (2001). Effects of Age on Tissues and Regions of the Cerebrum and Cerebellum. *Neurobiology of Aging*, vol.22, no.4, pp.581–594.
- Joe, B. N., Fukui, M. B., Meltzer, C. C., Huang, Q.-S., Day, R. S., Greer, P. J., and Bozik, M. E., (1999). Brain Tumor Volume Measurement: Comparison of Manual and Semiautomated Methods. *Radiology*, vol.212, no.3, pp.811–816.

- Joshi, J., (2010). Feature Extraction and Texture Classification in MRI. *Special Issue of IJCCT ;for International Conference (ICCT)*. pp. 130–136.
- Juang, L.-H., and Wu, M.-N., (2010). MRI Brain Lesion Image Detection Based on Color-Converted k-Means Clustering Segmentation. *Measurement*, vol.43, no.7, pp.941–949.
- Kadam, D. B., Gade, S. S., Uplane, M. D., and Prasad, R. K., (2011). Neural Network Based Brain Tumor Detection Using MR Images. *International Journal of Computer Science and Communication*, vol.2, no.2, pp.325–331.
- Kang, W. X., Yang, Q. Q., and Liang, R. R., (2009). The Comparative Research on Image Segmentation Algorithms. *First International Workshop on Education Technology and Computer Science (ETCS)*. IEEE, pp. 703–707.
- Kapur, T., Grimson, W. E., Wells, W. M., and Kikinis, R., (1996). Segmentation of Brain Tissue from Magnetic Resonance Images. *Medical Image Analysis*, vol.1, no.2, pp.109–127.
- Kasabov, N. K., (1998). *Foundations of Neural Networks, Fuzzy Systems, and Knowledge Engineering*. Second Edition. A Bradford Book. The MIT Press, Cambridge, Massachusetts, London, England.
- Kass, M., Witkin, A., and Terzopoulos, D., (1987). Snakes : Active Contour Models. *International Journal of Computer Vision*, vol.1, no.14, pp.321–331.
- Kattoush, A. H., (2012.) A Radon Slantlet Transforms Based OFDM System Design and Performance Simulation Under Different Channel Conditions. *ISRN Communications and Networking*, pp.1–8.
- Kharrat, A., Benamrane, N., Messaoud, M. B., and Abid, M., (2009). Detection of Brain Tumor in Medical Images. *3rd International Conference on Signals, Circuits and Systems (SCS)*. IEEE, pp. 1–6.
- Khotanlou, H., Colliot, O., Atif, J., and Bloch, I., (2009). 3D Brain Tumor Segmentation in MRI Using Fuzzy Classification, Symmetry Analysis and Spatially Constrained Deformable Models. *Elsevier, Fuzzy Sets and Systems*, vol.160, pp.1457–1473.
- Kikinis, R., Gleason, P. L., Moriarty, T. M., Moore, M. R., Alexander, E., Stieg, P. E., and Jolesz, F. A., (1996). Computer-Assisted Interactive Three-Dimensional Planning for Neurosurgical Procedures. *Neurosurgery*, vol.38, no.4, pp.640–651.

- Kikinis, R., Shenton, M. E., Gerig, G., Martin, J., Anderson, M., Metcalf, D., Guttmann, C. R., McCarley, R. W., Lorensen, W., Cline, H., and Jolesz, F. A., (1992). Routine Quantitative Analysis of Brain and Cerebrospinal Fluid Spaces With MR Imaging. *Journal of Magnetic Resonance Imaging*, vol.6, no.2, pp.619–629.
- Klein, S., Loog, M., Van-Der-Lijn, F., Den-Heijer, T., Hammers, A., De-Bruijne, M., Van-Der-Lugt, A., Duin, R. P. W., Breteler, M. M. B., and Niessen, W. J., (2010). Early Diagnosis of Dementia Based OnIntersubject Whole-Brain Dissimilarities. In *Biomedical Imaging: From Nano to Macro, IEEE International Symposium*, pp. 249–252.
- Kumari, R., (2013). SVM Classification an Approach on Detecting Abnormality in Brain MRI Images. *International Journal of Engineering Research and Applications (IJERA)*, vol.3, no.4, pp.1686–1690.
- Kuperman, V., (2000). *Magnetic Resonance Imaging: Physical Principles and Applications*. First Edition. Academic Press, Inc (London) LTD.
- Lacroix, M., Abi-Said, D., Fourney, D. R., Gokaslan, Z. L., Shi, W., DeMonte, F., and Sawaya, R., (2001). A Multivariate Analysis of 416 Patients With Glioblastoma Multiforme Prognosis Extent of Resection and Survival. *Journal of Neurosurgery*, vol.95, no.2, pp.190–198.
- Lakare, S., and Kaufman, A., (2000). 3D Segmentation Techniques for Medical Volumes. *Center for Visual Computing, Department of Computer Science, State University of NewYork*.
- Lalkhen, a. G., and McCluskey, A., (2008). Clinical Tests: Sensitivity and Specificity. *Continuing Education in Anaesthesia, Critical Care and Pain*, vol.8, no.6, pp.221–223.
- Lartizien, C., Marache-Francisco, S., and Prost, R., (2012). Automatic Detection of Lung and Liver Lesions in 3-D Positron Emission Tomography Images: A Pilot Study. *IEEE Transactions on Nuclear Science*, vol.59, no.1, pp.102–112.
- Latif, G., Kazmi, S. B., Jaffar, M. A., and Mirza, A. M., (2010). Classification and Segmentation of Brain Tumor Using Texture Analysis. *Recent Advances in Artificial Intelligence, Knowledge Engineering and Data Base*, pp.147–155.
- Lau, P. Y., Voon, F. C. T., and Ozawa, S., (2005). The Dtection and Visualization of Brain Tumors on T1-Weighted MRI Images Using Multiparameter Feature

- Blocks. *Proceedings of the 2005 IEEE Engineering in Medicine and Biology 27th Annual Conference Shanghai, China*. pp. 5104–5107.
- Lee, C., Huh, S., Ketter, T. A., Unser, M., (1998). Unsupervised Connectivity-Based Thresholding Segmentation of Midsagittal Brain MR Images. *Computers in Biology and Medicine*, vol.28, no.3, pp.309–338.
- Lee, K., (2009). Visualization of Multiresolution Model for Volumetric Medical Data by Using Weighted Alpha Shapes. *SPIE Medical Imaging. International Society for Optics and Photonics*, vol.7261, pp.1–8.
- Li, L., Rui, S., Nie, Q., Gong, X., and Li, F., (2012). Conformal Alpha Shape-Based Multi-Scale Curvature Estimation from Point Clouds. *Journal of Computers*, vol.7, no.6, pp.1460–1466.
- Liang, J., Edelsbrunner, H., Fu, P., Sudhakar, P. V., and Subramaniam, S., (1998). Analytical Shape Computation of Macromolecules: I. Molecular Area and Volume Through Alpha Shape. *Proteins Structure Function and Genetics*, vol.33, no.1, pp.1–17.
- Liang, J., and Dill, K. A., (2001). Are Proteins Well-Packed ? *Biophysical journal*, vol.81, no.2, pp.751–766.
- Lin, J., Cheng, K., and Mao, C., (1996). A Fuzzy Hopfield Neural Network for Medical Image Segmentation. *IEEE Transactions on Nuclear Science*, vol.43, no.4, pp.2389–2398.
- Lindeberg, T., and Li, M.-X., (1997). Segmentation and Classification of Edges Using Minimum Description Length Approximation and Complementary Junction Cues. *Computer Vision and Image Understanding*, vol.67, no.1, pp.88–98.
- Links, Jonathan, M., Lewis S. B., Baskaran, S., Matthew, A. R., Joseph, G. H., and Allan, L. R., (1998). Edge Complexity and Partial Volume Effects. *Journal Of Computer Assisted Tomography*, vol.22, no.3, pp.450–458.
- Logeswari, T., and Karnan, M., (2010). An Improved Implementation of Brain Tumor Detection Using Segmentation Based on Soft Computing. *Journal of Cancer Research and Experimental Oncology*, vol.2, no.1, pp.6–14.
- Logeswari, T., and Karnan, M., (2010). An Improved Implementation of Brain Tumor Detection Using Soft Computing. *Communication Software and Networks, ICCSN'10. Second International Conference, IEEE*. pp. 147–151.

- Lorenzen, P., Sarang, J., Guido, G., and Elizabeth, B., (2001). Tumor-Induced Structural and Radiometric Asymmetry in Brain Images. *Proceedings of the IEEE Workshop on Mathematical Methods in Biomedical Image Analysis (MMBIA '01)*. IEEE Computer Society, Washington, DC, USA, pp.163–170.
- Lou, S., Jiang, X., and Scott, P. J., (2013). Application of the Morphological Alpha Shape Method to the Extraction of Topographical Features from Engineering Surfaces. *Measurement*, vol.46, no.2, pp.1002–1008.
- Louis, D. N., Hiroko, O., Otmar, D. W., Webster, K. C., Peter, C. B., Anne, J., Bernd, W. S., and Paul, K., (2007). The 2007 WHO Classification of Tumours of The Central Nervous System. *Acta Neuropathologica*, vol.114, no.2, pp.97–109.
- Lucieer, A., and Kraak, M., (2004). α -Shapes for Visualizing Irregular Shaped Class Clusters in 3D. *Electronic Imaging 2004. International Society for Optics and Photonics*, pp.201–211.
- Lung, H. V., and Kim, J.-M., (2009). A Generalized Spatial Fuzzy c-Means Algorithm for Medical Image Segmentation. *Fuzzy Systems. FUZZ-IEEE . IEEE International Conference on*, pp. 409–414.
- Macdonald, David, R., Terrance, L. C., Schold, S. C., and Gregory, J. C., (1990). Response Criteria for Phase II Studies of Supratentorial Malignant Glioma. *Journal of Clinical Oncology*, vol.8, no.7, pp.1277–1280.
- Mallat, S. G., (1989). Multifrequency Channel Decompositions of Images and Wavelet Models. *Speech and Signal Processing, IEEE Transactions*, vol.37, no.12, pp.2091–2110.
- Mallat, S. G., (1989). A Theory for Multiresolution Signal Decomposition: The Wavelet Representation. *Pattern Analysis and Machine Intelligence, IEEE Transactions on*, vol.11, no.7, pp.674–693.
- Manousakas, I. N., Undrill, P. E., Cameron, G. G., and Redpath, T. W., (1998). Split-and-Merge Segmentation of Magnetic Resonance Medical Images: Performance Evaluation and Extension to Three Dimensions. *Computers and Biomedical Research*, vol.31, no.6, pp.393–412.
- Marian, W., (2008). *An Automated Modified Region Growing Technique for Prostate Segmentation in Trans Rectal Ultrasound Images*. Master's Thesis, Department of Electrical and Computer Engineering. University of Waterloo, Waterloo, Ontario, Canada.

- Mayr, N. A., Turgut, E. T., Yuh, B. P., Brown, B. C., Wen, R. E., Buller, B., Anderson, and Hussey, D. H., (1993). Cervical Cancer: Application of MR Imaging in Radiation Therapy. *Radiology*, vol.189, no.2, pp.601–608.
- Mayr, N. A., William, T. C., Yuh, J. Z., James, C. E., Joel, I. S., Vincent, A. M., Retta, E. P., and David, H. H., (1997). Tumor Size Evaluated by Pelvic Examination Compared With 3-D MR Quantitative Analysis in the Prediction of Outcome for Cervical Cancer. *International Journal of Radiation Oncology Biology Physics*, vol.39, no.2, pp.395–404.
- Mazziotta, J., Arthur, T., Alan, E., Peter, F., Jack, L., Karl, Z., Roger, W., (2001). A Probabilistic Atlas And Reference System for The Human Brain: International Consortium for Brain Mapping (ICBM). *Philosophical Transactions of the Royal Society of London. Series B: Biological Sciences* 356, vol.1412, pp.1293–1322.
- Mehmet, S., and Bulent, S., (2004). Survey Over Image Thresholding Techniques and Quantitative Performance Evaluation. *Journal of Electronic Imaging*, vol.13, no.1, pp.146–165.
- Mehmood, I., Naveed, E., Muhammad, S., and Sung, W. B., (2013). Prioritization of Brain MRI Volumes Using Medical Image Perception Model and Tumor Region Segmentation. *Computers in Biology and Medicine*, vol.43, no.10, pp.1471–1483.
- Meine, H., Köthe, U., and Stelldinger, P., (2009). A Topological Sampling Theorem for Robust Boundary Reconstruction and Image Segmentation. *Discrete Applied Mathematics*, vol.157, no.3, pp.524–541.
- Menze, B., and Leemput, K. Van, (2012). Segmenting Glioma in Multi-Modal Images using a Generative Model for Brain Lesion Segmentation. *Process MICCAI-BRATS (Multimodal Brain Tumor Segmentation Challenge)*, pp.49–55.
- Menze, B. H., Koen, V. L., Danial, L., Marc-André, W., Nicholas, A., and Polina, G., (2012). Segmenting Glioma in Multi-Modal Images Using a Generative-Discriminative Model for Brain Lesion Segmentation. *Process MICCAI-BRATS (Multimodal Brain Tumor Segmentation Challenge)*, pp.56–63.
- Merchant, Thomas, E., Ian, F. Pollack, and Jay S. L., (2010). Brain Tumors Across the Age Spectrum: Biology, Therapy, and Late Effects. *Seminars in Radiation Oncology*, vol.20, no.1, pp.58–66.

- Michael, W., (2010). *Probabilistic Modeling for Segmentation in Magnetic Resonance Images of the Human Brain*. First Edition. Logos Verlag Berlin GmbH.
- Mirajkar, G., and Barbadekar, B., (2010). Automatic Segmentation of Brain Tumors from MR Images Using Undecimated Wavelet Transform and Gabor Wavelets. *Electronics, Circuits, and Systems (ICECS), IEEE International Conference*. pp. 702–705.
- Mises, R. V., (1964). *Mathematical Theory of Probability and Statistics*. Second Edition. Academic Press, Inc (London) LTD.
- Moghaddam, M. J., and Soltanian-zadeh, H., (2011). Medical Image Segmentation Using Artificial Neural Networks. *Artificial Neural Networks-Methodological Advances and Biomedical Applications*, pp.121–138.
- Moon, N., Elizabeth B., Koen V. L., and GuidGo E., (2002). Model-Based Brain and Tumor Segmentation. *International Conference on Pattern Recognition, IEEE*. pp. 528–531.
- Moran, P. J., and Wagner, M., (1994). Introducing Alpha Shapes for the Analysis of Path Integral Monte Carlo Results. *Visualization'94, Proceedings., IEEE Conference, Computer Society Press*, pp. 52–59.
- Mustaqeem, A., Javed, A., and Fatima, T., (2012). An Efficient Brain Tumor Detection Algorithm Using Watershed and Thresholding Based Segmentation. *International Journal of Image, Graphics and Signal Processing*, vol.4, no.10, pp.34–39.
- Mutt, S. K., and Kumar, S., (2009). Secure Image Steganography Based on Slantlet Transform. *Proceeding of International Conference on Methods and Models in Computer Science (ICM2CS)*. IEEE, pp. 1–7.
- Narr, K. L., Paul, M. T., Philip, S., Delbert, R., Seonah, J., Roger, P. W., Sharon, K., (2004). Regional Specificity of Hippocampal Volume Reductions in First-Episode Schizophrenia. *NeuroImage*, vol.21, no.4, pp.1563–1575.
- Natarajan, P., Nikhil, K., Natasha, S. K., Saldanha, N., and Bhanu, P. S., (2012). Tumor Detection Using Threshold Operation in MRI Brain Images. *Computational Intelligence and Computing Research (ICCIC), IEEE International Conference*. pp. 1–4.
- Nelson, S. J., (2001). Analysis of Volume MRI and MR Spectroscopic Imaging Data for the Evaluation of Patients with Brain Tumors. *Magnetic Resonance in*

- Medicine*, vol.46, no.2, pp.228–239.
- Nikkilä, M., Polishchuk, V., and Krasnoshchekov, D., (2014). Robust Estimation of Seismic Coda Shape. *Geophysical Journal International*, pp.1–18.
- Noback, C. R., Strominger, N. L., Demarest, R. J., and Ruggiero, D. A., (2005). *The Human Nervous System Structure And Function*. Sixth Edition, New Jersey: Humana Press.
- Nolte, J., (2013). *The Human Brain in Photographs and Diagrams*. Fourth Edition. Elsevier-Health Sciences.
- Novelline, R. A., and Squire, L. F., (2004). *Squire's Fundamentals of Radiology*. Sixth Edition. United States of America: Harvard College.
- Okuda, T., Yukunori, K., Yoshinori, S., Takeshi, S., Toshinori, H., Ichiro, I., Luxia, L., and Mutsumasa, T. M. D., (1999). Brain Lesions: When Should Recovery Sequences Be Used in MR Evaluation?. *Radiology*, v10.112, no.3, pp.793–798.
- Ortiz, A., Górriz, J. M., Ramirez, J. and Salas-Gonzalez, D., (2011). MR Brain Image Segmentation By Growing Hierarchical SOM and Probability Clustering. *Electronics Letters*, vol.47, no.10, pp.585–586.
- Otsu, N., (1979). A Threshold Selection Method from Gray-Level Histograms. *IEEE Transactions on Systems, Man, and Cybernetics*, vol.9, no.1, pp.62–66.
- Ozkan, M., Dawant, B. M., and Maciunas, R. J., (1993). Neural-Network-Based Segmentation of Multi-Modal Medical Images: A Comparative and Prospective Study. *Medical Imaging, IEEE Transactions*, vol.12, no.3, pp.534–544.
- Padma, A., (2011). A Wavelet Based Automatic Segmentation of Brain Tumor in CT Images Using Optimal Statistical Texture Features. *International Journal of Image Processing (IJIP)*, pp.552–563.
- Padma, A., and Sukanech, R., (2011). Texture Feature Based Analysis of Segmenting Soft Tissues from Brain CT Images Using BAM Type Artificial Neural Network. *Journal of Information Engineering and Applications*, vol.1, no.4, pp.34–44.
- Padma, A., and Sukanesh, R., (2011). Automatic Classification and Segmentation of Brain Tumor in CT Images using Optimal Dominant Gray level Run length Texture Features. *International Journal of Advanced Computer Science and Application*, vol.2, no.10, pp.53–59.

- Park, J. G., and Lee, C., (2009). Skull Stripping Based on Region Growing for Magnetic Resonance Brain Images. *NeuroImage*, vol.47, no.4, pp.1394–1407.
- Park, S. H., Lee, S. S., and Kim, J. H., (2005). A Surface Reconstruction Algorithm Using Weighted Alpha Shapes. *Fuzzy Systems and Knowledge Discovery. Springer Berlin Heidelberg*, pp.1141–1150.
- Pérot, S., Olivier, S., Maria, A. M., Anne-Claude, C., and Bruno O. V., (2010). Druggable Pockets and Binding Site Centric Chemical Space: a Paradigm Shift in Drug Discovery. *Drug Discovery Today*, vol.15, no.15, pp.656–667.
- Pesaresi, L., and Schwingshackl, C. W., (2014). Automated Measurement Grid Generation for Scanning Laser Doppler Vibrometers. *Topics in Modal Analysis, Springer New York*, vol.7, pp.645–653.
- Pohle, R., and Toennies, K. D., (2001). Segmentation of Medical Images Using Adaptive region Growing. *Medical Imaging. International Society for Optics and Photonics.*, pp.1337–1346.
- Polidais, (2006). Medical Imaging in Cancer Care : Charting The Progress. *US Oncology and National Electrical Manufacturers Association (NEMA)*, pp.1–32.
- Pradhan, N., and Sinha, A. K., (2011). Fuzzy ANN Based Detection and Analysis of Pathological and Healthy Tissues in Flair Magnetic Resonance Images. *International Journal of Information Technology and Knowledge Management*, vol.4, no.2, pp.471–476.
- Prastawa, M., Elizabeth, B., Sean, H., and Guido, G., (2004). A Brain Tumor Segmentation Framework Based on Outlier Detection. *Medical Image Analysis*, vol.8, no.3, pp.275–283.
- Prastawa, M., and Gerig, G., (2008). Automatic MS Lesion Segmentation By Outlier Detection and Information Theoretic Region Partitioning. Grand Challenge Work.: Multiple Sclerosis. Lesion Segmentation. Challenge, pp.1–8.
- Quinn, S. D., John, V., Erika, K., Wadyslaw, G., and Lesley, R., (2013). Measurement of Uterine Fibroid Volume a Comparative Accuracy and Validation of Methods Study. *European Journal of Obstetrics and Gynecology and Reproductive Biology*, vol. 71, no.1, pp.161–165.
- Rajendran, A., and Dhanasekaran, R., (2011). A Hybrid Method Based on Fuzzy Clustering and Active Contour Using GGVF for Brain Tumor Segmentation on MRI Images. *European Journal of Scientific Research*, vol.61, no.2,

pp.305–313.

- Rastgarpour, M., and Shanbehzadeh, J., (2011). Application of AI Techniques in Medical Image Segmentation and Novel Categorization of Available Methods and Tools. *Proceedings of the International Multi Conference of Engineers and Computer Scientists (IMECS), Hong Kon*, vol.1, pp.1-6
- Raviv, T. R., Leemput, K. Van, and Menze, B. H., (2012). Multi-Modal Brain Tumor Segmentation via Latent Atlases. *Process MICCAI-BRATS (Multimodal Brain Tumor Segmentation Challenge)*, pp.64–73.
- Reddy, K. K., Solmaz, B., Yan, P., Avgeropoulos, N. G., Rippe, D. J., and Shah, M., (2012). Confidence Guided Enhancing Brain Tumor Segmentation in Multi-Parametric MRI. *IEEE International Symposium on Biomedical Imaging (ISBI)*, pp.366–369.
- Rehm, K., Rehm, K., Schaper, K., Anderson, J., Woods, R., Stoltzner, S., and Rottenberg, D., (2004). Putting Our Heads Together: a Consensus Approach to Brain/Non-Brain Segmentation in T1-Weighted MR Volumes. *NeuroImage*, vol.22, no.3, pp.1262–1270.
- Rex, D. E., Rex, D. E., Shattuck, D. W., Woods, R. P., Narr, K. L., Luders, E., Rehm, K., Stoltzner, S. E., Rottenberg, D. A., and Toga, A. W., (2004). A Meta-Algorithm for Brain Extraction in MRI. *NeuroImage*, vol.23, no.2, pp.625–637.
- Rioul, Olivier, and Vetterli, M., (1991). Wavelets and Signal Processing. *IEEE Signal Processing Magazine*, 8 (LCAV-ARTICLE-1991-005), pp.14–38.
- Rohs, R., Rohs, R., West, S. M., Sosinsky, A., Liu, P., Mann, R. S., and Honig, B., (2009). The Role of DNA Shape in Protein - DNA Recognition. *Nature*, pp.1248–1253.
- Roland, P. E., (1993). *Brain Activation*. First Edition. New York, USA: Wiley-Liss.
- Rother, K., Hildebrand, P. W., Goede, A., Gruening, B., and Preissner, R., (2009). Voronoia: Analyzing Packing in Protein Structures. *Nucleic acids research*, vol.37, pp.393–395.
- Rousseau, François, H., Piotr, A., and Studholme, C., (2012). A Supervised Patch-Based Approach for Human Brain Labeling. *Medical Imaging, IEEE Transactions*, vol.30, no.10, pp.1852–1862.
- Rousseau, F., Habas, P.A., and Studholme, C., (2011). Human Brain Labeling Using Image Similarities. *Computer Vision and Pattern Recognition (CVPR), IEEE*

Conference. pp. 1081–1088.

- Roy, S., Nag, S., Maitra, I. K., Samir, P., and Bandyopadhyay, K., (2013). A Review on Automated Brain Tumor Detection and Segmentation from MRI of Brain. *ArXiv Preprint ArXiv*, vol.1, no.1, pp.1–41.
- Ruan, S., Jaggi, C., Xue, J., Fadili, J., and Bloyet, D., (2000). Brain Tissue Classification of Magnetic Resonance Images Using Partial Volume Modeling. *IEEE Transactions on Medical Imaging*, vol.19, no.12, pp.79–87.
- Rusinek, Henry, Leon, M. J. d., George, A. E., Stylopoulos, L. A., Chandra, R., Smith, G., Rand, T., Mourino, M., and Kowalski, H., (1991). Alzheimer Disease Measuring Loss of Cerebral Gray Matter With MR Imaging. *Radiology*, vol.178, no.1, pp.109–114.
- Sadanathan, A. S., Zheng, W., Chee, M. W., and Zagorodnov, V., (2010). Skull Stripping Using Graph Cuts. *NeuroImage*, vol.49, no.1, pp.225–239.
- Salankar, S. S., and Bora, V. R., (2014). MRI Brain Cancer Classification Using Support Vector Machine. *Electrical, Electronics and Computer Science (SCEECs), IEEE Students' Conference*. pp. 1–6.
- Salman, Y. M., Assal, M. A., Badawi, A. M., Alian, S. M., and El-Bayome, M., (2005). Validation Techniques for Quantitative Brain Tumors Measurements. *Engineering in Medicine and Biology Society. IEEE-EMBS. 27th Annual International Conference. IEEE*. pp. 7048–7051.
- Sasikala, M., Kumaravel, N., and Subhashini, L., (2006). Automatic Tumor Segmentation Using Optimal Texture Features. *IET 3rd International Conference on Advances in Medical, Signal and Information Processing, MEDSIP*. pp. 1–4.
- Sato, M., Lakare, S., Wan, M., Kaufman, A., and Nakajima, M., (2000). A Gradient Magnitude Based Region Growing Algorithm for Accurate Segmentation. *Image Processing. International Conference. IEEE*, vol.3, pp. 448–451.
- Schenone, A., Firenze, F., Acquarone, F., Gambaro, M., Masullif, F., and Andreucci, L., (1996). Segmentation of Multivariate Medical Images via Unsupervised Clustering With “Adaptive Resolution”. *Computerized Medical Imaging and Graphics*, vol.20, no.3, pp.119–129.
- Schmidt, M., and Murtha, A., (2005). Segmenting Brain Tumors Using Alignment-Based Features. *Machine Learning and Applications. Proceedings. Fourth International Conference, IEEE*. pp. 1–6.

- Sebastian, and García, M. T., (2007). Neuroimage Experimental Data Base Resources. *Grupo de Inteligencia Computacional, UPV/EHU Contents*, pp.1–17.
- Ségonne F., Dale, A. M., Busa, E., Glessner, M., Salat, D., Hahn, H. K., and Fischl, B., (2004). A Hybrid Approach to the Skull Stripping Problem in MRI. *NeuroImage*, vol.22, no.3, pp.1060–1075.
- Selesnick, I. W., (1999). The Slantlet Transform. *IEEE Transactions on Signal Processing*, vol.47, no.5, pp.1304–1313.
- Selvaraj, H., Selvi, S. T., Selvathi, D., and Gewali, L., (2007). Brain MRI Slices Classification Using Least Squares Support Vector Machine. *International Journal of Intelligent Computing in Medical Sciences and Image Processing*, vol.1, no.1, pp.21–33.
- Shally, H., and Chitharanjan, K., (2013). Tumor Volume Calculation of Brain from MRI Slices. *International Journal of Computer Science and Engineering Technology (IJCSET)*, vol.4, no.8, pp.1126–1132.
- Sharma, J., Sanfilipo, M. P., Benedict, R. B., Weinstock-guttman, B., Frederick E. M., and Bakshi, R., (2004). Whole-Brain Atrophy in Multiple Sclerosis Measured by Automated versus Semiautomated MR Imaging Segmentation. *American Journal of Neuroradiology*, vol.25, no.6, pp.985–996.
- Shattuck, D. W., Sandor-Leahy, S. R., Schaper, K. A., Rottenberg, D. A., and Leahy, R. M., (2001). Magnetic Resonance Image Tissue Classification Using a Partial Volume Model. *NeuroImage*, vol.13, no.5, pp.856–876.
- Shi, W. M., Wildrick, D. M., and Sawaya, R., (1998). Volumetric Measurement of Brain Tumors from MR Imaging. *Journal of Neuro-Oncology*, vol.37, no.1, pp.87–93.
- Shin, H., (2012). Hybrid Clustering and Logistic Regression for Multi-Modal Brain Tumor Segmentation. *Process MICCAI-BRATS (Multimodal Brain Tumor Segmentation Challenge)*, pp.32–35.
- Siegel, R. Desantis, C., Virgo, K., Stein, K., Mariotto, A., Smith, T., Cooper, D., Gansler, T., Lerro, C., and Fedewa, S., (2012). Cancer Treatment and Survivorship Statistics, 2012. *CA: A Cancer Journal for Clinicians*, vol.62, no.4, pp.220–241.
- Sikka, K., Sinha, N., Singh, P. K., and Mishra, A. K., (2009). A Fully Automated Algorithm Under Modified FCM Framework for Improved Brain MR Image

- Segmentation. *Magnetic Resonance Imaging*, vol.27, no.7, pp.994–1004.
- Singh, D., and Kaur, K., (2012). Classification of Abnormalities in Brain MRI Images Using GLCM , PCA and SVM. *International Journal of Engineering and Advanced Technology (IJEAT)*, vol.1, no.6, pp.243–248.
- Singh, L., Dubey, R. B., Jaffery, Z. A., and Zaheeruddin, Z., (2009). Segmentation and Characterization of Brain Tumor from MR Images. *ARTCom 2009 - International Conference on Advances in Recent Technologies in Communication and Computing. IEEE*, pp. 815–819.
- Sinha, K. and Sinha, G. R., (2014). Efficient Segmentation Methods for Tumor Detection in MRI Images. *Electrical, Electronics and Computer Science (SCEECS), IEEE Students' Conference*, pp. 1–6.
- Smirniotopoulos and James, G., (1999). The New WHO Classification of Brain Tumors. *Neuroimaging*, vol.9, no.4, pp.595–613.
- Smith, C. J., (2012). Diagnostic Tests (1) - Sensitivity and Specificity. *Phlebology / Venous Forum of the Royal Society of Medicine*, vol.27, no.5, pp.250–251.
- Smith, S. M., (2002). Fast Robust Automated Brain Extraction. *Human Brain Mapping*, vol.17, no.3, pp.143–155.
- Soesanti, I., Susanto, A., Widodo, T. S., and Tjokronagoro, M., (2011). MRI Brain Images Segmentation Based on Optimized Fuzzy Logic and Spatial Information. *International Journal of Video and Image Processing and Network Security*, vol.11, no.4, pp.6–11.
- Somasundaram, K. and Kalaiselvi, T., (2011). Automatic Brain Extraction Methods for T1 Magnetic Resonance Images Using Region Labeling and Morphological Operations. *Computers in Biology and Medicine*, vol.41, no.8, pp.716–725.
- Somasundaram, K. and Kalaiselvi, T., (2010). Automatic Detection of Brain Tumor from MRI Scans Using Maxima Transform. *UGC Sponsored National Conference on Image Processing-NCIMP*. pp. 136–141.
- Somasundaram, K. and Kalavathi, P., (2011). *Medical Image Binarization Using Square Wave Representation*. First Edition. Springer-Verlag Berlin Heidelberg.
- Stippich, C., (2007). *Clinical Functional MRI*. First Edit. Germany: Springer-Verlag Berlin Heidelberg.

- Strother, S., La-Conte, S., Kai-Hansen, L., Anderson, J., Zhang, J., Pulapura, S., and Rottenberg, D., (2004). Optimizing the fMRI Data-Processing Pipeline Using Prediction and Reproducibility Performance Metrics: I. A Preliminary Group Analysis. *NeuroImage*, vol.23, pp.196–207.
- Subbanna, N. K. and Arbel, T., (2012). Probabilistic Gabor and Markov Random Fields Segmentation of Brain Tumours in MRI Volumes. *Process MICCAI-BRATS (Multimodal Brain Tumor Segmentation Challenge)*, pp.28–31.
- Sullivan, J. M., Charron, G. and Paulsen, K. D., (1997). A Three-Dimensional Mesh Generator for Arbitrary Multiple Material Domains. *Finite Elements in Analysis and Design*, vol.25, no.3, pp.219–241.
- Suri, J. S., (2001). Two-Dimensional Fast Magnetic Resonance Brain Segmentation. *Engineering in Medicine and Biology Magazine*, vol.20, no.4, pp.84–95.
- Tanskanen, P., Veijola, J. M., Piippo, U. K., Haapea, M., Miettunen, J. A., Pyhtinen, J., Bullmore, E. T., Jones, P. B., and Isohanni, M. K., (2005). Hippocampus and Amygdala Volumes in Schizophrenia and other Psychoses in the Northern Finland 1966 Birth Cohort. *Schizophrenia research*, vol.75, no.2, pp.283–294.
- Teichmann, M. and Capps, M., (1998). Surface Reconstruction With Anisotropic Density-Scaled Alpha Shapes. *Visualization '98. Proceedings*, pp.67–72.
- Thompson, P. M., Mega, M. S., Woods, R. P., Zoumalan, C. I., Lindshield, C. J., Blanton, R. E., Moussai, J., Holmes, C. J., Cummings, J. L., and Toga, A. W., (2001). Cortical Change in Alzheimer's Disease Detected with a Disease-Specific Population-Based Brain Atlas. *Cerebral Cortex*, vol.11, no.1, pp.1–16.
- Tian, G., Xia, Y., Zhang, Y., and Feng, D., (2011). Hybrid Genetic and Variational Expectation-Maximization Algorithm for Gaussian-Mixture-Model-Based Brain MR Image Segmentation. *Information Technology in Biomedicine, IEEE Transactions*, vol.15, no.3, pp.373–380.
- Toga, A. W., (1999). *Brain Warping*. First Edition. Academic Press, Inc (London) LTD.
- Tomas-Fernandez, X. and Warfiel, S. K., (2012). Automatic Brain Tumor Segmentation Based on a Coupled Global-Local Intensity Bayesian Model. *Process MICCAI-BRATS (Multimodal Brain Tumor Segmentation Challenge)*, pp.41–48.

- Tommaso, S., (2012). *Imaging Gliomas After Treatment*. First Edit. Milan, Italia: Springer.
- Veloz, A., Orellana, A. and Vielma, J., (2011). Brain Tumors : How Can Images and Segmentation Techniques Help? *Diagnostic Techniques and Surgical Management of Brain Tumors*, pp.67–92.
- Venkatesh, S. S., (2013). *The Theory of Probability: Explorations and Applications*. First Edit., United Kingdom, Cambridge: Cambridge University Press.
- Vijayakumar, B. and Chaturvedi, A., (2013). Brain Tumor In Three Dimensional Magnetic Resonance Images and Concavity Analysis. *International Journal of Computer Application*, vol.1, no.3, pp.1–84.
- Wakchaure, S. L., Ghuge, G. D., and Musale., D. S., (2014). The Detection and Visualization of Brain Tumors on T1-Weighted MRI Images Using Multiparameter Feature Blocks. *International Journal of Emerging Technology and Advanced Engineering*, vol.4, no.2, pp.127–131.
- Wang, Y., Lin, Z. X., Cao, J. G., Li, M. Q., (2011). Automatic MRI Brain Tumor Segmentation System Based on Localizing Active Contour Models. *Advanced Materials Research*, 219-220, pp.1342–1346.
- Weizman, L., Ben Sira, L., Joskowicz, L., Constantini, S., Precel, R., Shofty, B., and Ben Bashat, D., (2012). Automatic Segmentation, Internal Classification, and Follow-Up of Optic Pathway Gliomas in MRI. *Medical Image Analysis*, vol.16, no.1, pp.177–188.
- Weizman, L., Sira, L. B., Joskowicz, L., Rubin, D. L., Yeom, K. W., Constantini, S., Shofty, B. B., and Dafna, B., (2014). Semiautomatic Segmentation and Follow-Up of Multicomponent Low-Grade Tumors in Longitudinal Brain MRI Studies. *Medical Physics*, vol.41, no.5, p.052303.
- Wels, M., Carneiro, G., Aplas, A., Huber, M., Hornegger, J., and Comaniciu, D., (2008). A Discriminative Model-Constrained Graph Cuts Approach to Fully Automated Pediatric Brain Tumor Segmentation in 3-D MRI. *International Conference on Medical Image Computing and Computer-Assisted Intervention : MICCAI*, pp. 67–75.
- Wilson, J. A., Bender, A., Kaya, T., Clemons, P. A., (2009). Alpha Shapes Applied to Molecular Shape Characterization Exhibit Novel Properties Compared to Established Shape Descriptors. *Journal of Chemical Information and Modeling*, vol.49, no.10, pp.2231–2241.

- Wong, K. K. L., Sun, Z., Tu, J., Worthley, S. G., Mazumdar, J., and Abbott, D., (2012). Medical Image Diagnostics Based On Computer-Aided Flow Analysis Using Magnetic Resonance Images. *Computerized Medical Imaging and Graphics*, vol.36, no.7, pp.527–541.
- Woods, R.P., Grafton, S. T., Watson, J. D., Sicotte, N. L., Mazziotta, J. C., (1998). Automated Image Registration: II . Intersubject Validation of Linear and Nonlinear Models. *Journal of Computer Assisted Tomography*, vol.22, no.1, pp.153–165.
- Woods, R. P., Dapretto, M., Sicotte, N. L., Toga, A. W., and Mazziotta, J. C., (1999). Creation and Use of a Talairach-Compatible Atlas for Accurate, Automated, Nonlinear Intersubject Registration, and Analysis of Functional Imaging Data. *Human Brain Mapping*, vol.8, no.2, pp.73–79.
- Wright, A., (2010). Brain Scanning Techniques (CT, MRI, fMRI, PET, SPECT, DTI, DOT). *Cerebra Positively Different*, pp.1–14.
- Wu, J., Ye, F., Ma, J.-l., Sun, X.-P., Xu, J., and Cui, Z.-M., (2008). The Segmentation and Visualization of Human Organs Based on Adaptive Region Growing Method. *Computer and Information Technology Workshops. CIT Workshops. IEEE 8th International Conference*. pp. 439–443.
- Xavierarockiaraj, S., Nithya, K. and Devi, R. M., (2012). Brain Tumor Detection Using Modified Histogram Thresholding-Quadrant Approach. *Journal of Computer Applications (JCA)*, vol.5, no.1, pp.21–25.
- Xiao, Y. and Hu, J., (2012). Hierarchical Random Walker for Multimodal Brain Tumor Segmentation. *Process MICCAI-BRATS (Multimodal Brain Tumor Segmentation Challenge)*, pp.36–40.
- Xu, R., Luo, L. and Ohya, J., (2002). Segmentation of Brain MRI. *Advances in Brain Imaging. Rijeka, Croatia: InTech*, pp.143–169.
- Yoo, Y., (2001). Tutorial on Fourier Theory. *Retrieved*, pp.1–18.
- Yousefi, S., Kehtarnavaz, N. and Gholipour, A., (2012). Improved Labeling of Subcortical Brain Structures in Atlas-Based Segmentation of Magnetic. *Biomedical Engineering, IEEE Transactions*, vol.59, no.7, pp.1808–1817.
- Zacharaki, E. I., Wang, S., Chawla, S., Yoo, D. S., Wolf, R., Melhem, E. R., and Davatzikos, C., (2009). MRI-Based Classification Of Brain Tumor Type and Grade Using SVM-RFE. *Biomedical Imaging: From Nano to Macro, ISBI'09. IEEE International Symposium*, pp.1035–1038.

- Zacharaki, E. I., Shen, D., Lee, S.-K., and Davatzikos, C., (2008). ORBIT: A Multiresolution Framework for Deformable Registration of Brain Tumor Images. *IEEE Transactions on Medical Imaging*, vol.27, no.8, pp.1003–1017.
- Zeng, X., Staib, L. H., Schultz, R. T., and Duncan, J. S., (1999). Segmentation and Measurement of the Cortex from 3-D MR Images Using Coupled-Surfaces Propagation. *IEEE Transactions on Medical Imaging*, vol.18, no.10, pp.927–937.
- Zhang, N., Ruan, S., Lebonvallet, S., Liao, Q., and Zhu, Y., (2011). Kernel Feature Selection to Fuse Multi-Spectral MRI Images for Brain Tumor Segmentation. *Computer Vision and Image Understanding*, vol.115, no.2, pp.256–269.
- Zhang, N., Liao, Q. and Lyon, I. D., (2009). Multi-kernel SVM Based Classification for Tumor Segmentation by Fusion of MRI Images. *Imaging Systems and Techniques, IST'09. IEEE International Workshop*, pp.71–75.
- Zhang, T., Xia, Y. and Feng, D. D., (2012). Clonal Selection Algorithm for Gaussian Mixture Model Based Segmentation of 3D Brain MR Images. *Intelligent Science and Intelligent Data Engineering. Springer Berlin Heidelberg.*, pp.295–302.
- Zhang, Y., Dong, Z., Wu, L., and Wang, S., (2011). A Hybrid Method for MRI Brain Image Classification. *Expert Systems with Applications*, vol.38, no.8, pp.10049–10053.
- Zhang, Y., Qu, H. and Wang, Y., (1994). Adaptive Image Segmentation Based on Fast Thresholding and Image Merging. *Artificial Reality and Telexistence-Workshops*, pp.308–311.
- Zhao, J., Shao, F. Q., Zhang, X. D., and Feng, C., (2012). An Improved Integrated Active Contour Model without Re-Initialization for Vector-Valued Images Segmentation. *Advanced Materials Research*, vol.429, pp.271–276.
- Zhao, L., Wu, W. and Corso, J. J., (2012). Brain Tumor Segmentation Based on GMM and Active Contour Method with a Model-Aware Edge Map. *Process MICCAI-BRATS (Multimodal Brain Tumor Segmentation Challenge)*, pp.24–27.
- Zhou, J., Chan, K. L., Chong, V. F., and Krishnan, S. M., (2005). Extraction of Brain Tumor From MR Images Using One-Class Support Vector Machine. *Annual International Conference of the IEEE Engineering in Medicine and Biology Society*. pp. 6411–6414.

- Zhou, W. and Yan, H., (2014). Alpha Shape and Delaunay Triangulation in Studies of Protein-Related Interactions. *Briefings in Bioinformatics*, vol.15, no.1, pp.54–64.
- Zhou, W. and Yan, H., (2010). Prediction of DNA-Binding Protein Based on Alpha Shape Modeling. *IEEE International Conference on Bioinformatics and Biomedicine (BIBM)*, pp. 23–28.
- Zhou, W. and Yan, H., (2010). Relationship Between Periodic Dinucleotides and the Nucleosome Structure Revealed by Alpha Shape Modeling. *Chemical Physics Letters*, vol.489, no.4, pp.225–228.
- Zhou, W., Yan, H. and Hao, Q., (2012). Analysis of Surface Structures of Hydrogen Bonding in Protein - Ligand Interactions Using the Alpha Shape Model. *Chemical Physics Letters*, vol.545, pp.125–131.
- Zhu, S. C. and Yuille, A., (1996). Region Competition: Unifying Snakes, Region Growing and Bayes/MDL for Multiband Image Segmentation. *Pattern Analysis and Machine Intelligence, IEEE Transactions*, vol.18, no.9, pp.884–900.
- Zhuang, A. H., Valentino, D. J. and Toga, A. W., (2006). Skull-Stripping Magnetic Resonance Brain Images Using a Model-Based Level Set. *NeuroImage*, vol.32, no.1, pp.79–92.
- Zikic, D., Glocker, B., Konukoglu, E., and Shotton, J., (2012). Context-Sensitive Classification Forests for Segmentation of Brain Tumor Tissues. *Process MICCAI-BRATS (Multimodal Brain Tumor Segmentation Challenge)*, pp.1–9.
- Zivadinov, R., Bagnato, F., Nasuelli, D., Bastianello, S., Bratina, A., Locatelli, L., Watts, K., Finamore, L., Grop, A., Dwyer, M., Catalan, M., Clemenzi, A., Millefiorini, E., Bakshi, R., and Zorzon, M., (2004). Short-Term Brain Atrophy Changes In Relapsing-Remitting Multiple Sclerosis. *Journal of the Neurological Sciences*, vol.223, no.2, pp.185–193.
- Zomorodian, A., Guibas, L. and Koehl, P., (2006). Geometric Filtering of Pairwise Atomic Interactions Applied to the Design of Efficient Statistical Potentials. *Computer Aided Geometric Design*, vol.23, no.6, pp.531–544.